REPORT 1277

INTERACTION OF A FREE FLAME FRONT WITH A TURBULENCE FIELD[1]

By Maurice Tucker

SUMMARY

Small-perturbation spectral-analysis techniques are used to obtain the root-mean-square flame-generated turbulence velocities and the attenuating pressure fluctuations stemming from interaction of a constant-pressure flame front with a field of isotropic turbulence in the absence of turbulence decay processes.

The anisotropic flame-generated turbulence velocities are found to be of about the same intensity as those of the incident isotropic turbulence, the lateral turbulence velocities being always lower, but the longitudinal velocity is somewhat increased for flame-temperature ratios over 7. The small-perturbation analysis indicates that the incremental turbulent flame speed is a second-order quantity composed of two parts. One part represents the root-mean-square area of the turbulent flame front; the other represents the contribution of the transverse velocity fluctuations resulting from the flame-front distortion. Directly at the flame front, the noise-pressure levels of the pressure fluctuations are fairly intense (59 to 81 db referred to 0.0002 dyne/sq cm) even at moderate approach-flow turbulence intensities.

INTRODUCTION

Development of high-output jet engines has stimulated interest in the role played by turbulence in combustion phenomena. In the earliest studies of flame-turbulence interaction, Damkohler (ref. 1) and Shelkin (ref. 2) utilized mixing-length theories of turbulence to obtain semiquantitative relations for predicting flame speeds. Damkohler introduced the concept that turbulence of a scale large relative to the flame-front thickness increases the average flame speed by increasing the instantaneous flame surface area. The relations of references 1 and 2 were not confirmed by the experimental values of turbulent flame speed in Bunsen burners obtained in reference 3. Experiments on flames stabilized in channels (ref. 4) suggested that approach-flow turbulence had little effect on burning velocity and that the disturbances affecting turbulent flame speed were primarily flame-generated. A similar conclusion was drawn in reference 5.

In an attempt to obtain agreement between theory and experiment, Karlovitz, Denniston, and Wells (ref. 6) and Scurlock and Grover (ref. 7) have incorporated the concept of flame-generated disturbances in their recent theories of turbulent flame speed which utilize G. I. Taylor's one-dimensional theory of diffusion by continuous movements. The somewhat arbitrary assumption is made in the analyses of both references 6 and 7 that these flame-generated disturbances constitute additional turbulence only. In reference 6 the energy of the flame-generated turbulence is taken as the difference between the kinetic energy of the burned gas in the absence of turbulence and the kinetic energy obtained by using the average velocity of the burned gas normal to the turbulent flame front. In reference 7 the flame-generated turbulence energy is obtained from a momentum balance of unburned and burned gases before and after an assumed mixing of the burned gas.

The data obtained in reference 8 on pentane-air flames baffle-stabilized in a rectangular duct suggest that the methods of references 6 and 7 considerably overestimate the turbulence generated by flame-turbulence interaction. Apart from the question of validity of such methods of calculating flame-generated turbulence, objections have been raised (ref. 9) to calculations of flame speed made on the basis of a hypothetical upstream turbulence compounded from approach-stream turbulence and turbulence generated downstream of the flame as was done in reference 7 and implied in reference 6.

The present analysis is primarily concerned with the turbulence velocities and other fluctuation quantities associated with the linearized interaction of a free flame (not influenced by bounding walls) with turbulence present in the combustible mixture. Such turbulence will be referred to as approach-flow turbulence. The flame is treated as a discontinuity specified by the appropriate fundamental (laminar) flame speed and flame temperature. The interaction of such a flame front with a transverse plane wave, that is, a vorticity wave or shear wave, of arbitrary inclination relative to the front is first analyzed. The effects of an entire spectrum of transverse plane waves constituting a weak field of turbulence are then developed from the single-wave results. The statistical or root-mean-square fluctuation quantities describing the pressure fields and the anisotropic flame-generated turbulence resulting from interaction of the flame front with isotropic approach-flow turbulence are obtained for the limiting case of constant-pressure combustion. Some discussions of turbulent flame speed and of combustion noise are also presented.

[1] Supersedes NACA TN 3407, "Interaction of a Free Flame Front with a Turbulence Field," by Maurice Tucker, 1955.

435875—57——30

FLAME—TURBULENCE INTERACTION PROCESS

Turbulent motion may be regarded as a Fourier superposition of a very large number of different-sized and randomly oriented component plane-wave motions. The customary assumptions concerning the turbulence (see ref. 10) are also made in the present analysis, namely, that turbulent decay effects are negligible and that the density fluctuations associated with the turbulence are also small enough to be neglected. The first assumption, which implies inviscid flow and very small turbulent velocity fluctuations, permits linear superposition of the component waves. With the second assumption, the continuity equation requires that these Fourier waves be transverse plane waves, that is, vorticity or shear waves. For each of these waves the local velocity vector $\underline{A}$ is perpendicular to the vector $\underline{k}$, normal to the wave front. The vector $\underline{k}$ is termed the wave-number vector; its magnitude k is termed the wave number, which is defined as 2π divided by the wavelength. All symbols are defined in appendix A. Any one of the parallel planes containing both the local velocity vector $\underline{A}$ and the wave-number vector $\underline{k}$ is called the "polarization plane."

Because of the assumed linear superposition of the component waves, the complete interaction results can be obtained from the study of the interaction of a plane flame front with a single-component transverse wave of the turbulence field. For simplicity, this typical vorticity wave will first be taken as a two-dimensional wave. Generalization to the three-dimensional case will be made later. The configuration considered is shown in sketch (a):

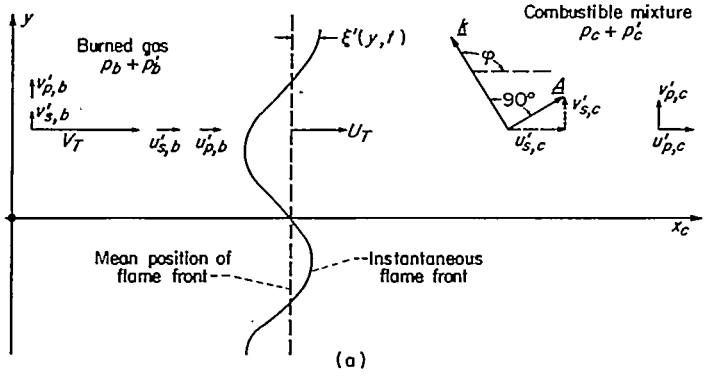

A flame front moves with mean velocity U_T into an inviscid combustible mixture. This mixture is at rest, but contains a vorticity wave with velocity vector $\underline{A}$ (components $u'_{s,c}$ and $v'_{s,c}$) and with wave-number vector $\underline{k}$ inclined at an angle φ to the positive direction of the x_c-axis. In the absence of any perturbation interaction, the plane front propagates into the combustible mixture with velocity U (the laminar flame speed). As indicated in appendix B, the motion of the burned gas, whose velocity V is constant, is away from the flame front. The flame front is assumed to be of infinite extent in directions transverse to the direction of the x_c-axis.

A weak inviscid disturbance field may be resolved into a stationary component and a moving component, both relative to the mean local flow (refs. 11 and 12). The moving component is an irrotational isentropic pressure-velocity disturbance. The stationary component, which is convected by the mean local flow, is a constant-pressure disturbance containing any vorticity fluctuations and entropy fluctuations present in the disturbance field. Thus, the interaction of the flame front with the vorticity wave would be expected to generate both an irrotational disturbance with velocity components $u'_{p,b}$, $v'_{p,b}$ and a rotational disturbance with velocity components $u'_{s,b}$, $v'_{s,b}$ in the burned gas, and an irrotational disturbance with velocity components $u'_{p,c}$, $v'_{p,c}$ in the combustible mixture. The resulting velocity fluctuations, which include both the irrotational and rotational disturbances, are designated as u'_c, v'_c and u'_b, v'_b for the combustible mixture and the burned gas, respectively. The flame front is displaced by an amount $\xi'(y,t)$ from its mean or unperturbed position as a result of the interaction.

The diagrams of figure 1, which are similar to those used in reference 12, may prove helpful in visualizing the interaction process. Suppose that at some instant t_1 the flame intersects a front of the vorticity wave at point P_1 of figure 1(a). At a later time $t_1+\delta t$, the flame has moved a distance $U\delta t$ and now intersects the stationary vorticity wave front at point P_2. A vorticity wave with front parallel to line QP_2 is then produced in the burned gas. A cylindrical sound wave is generated at point P_1 at time t_1 and propagates at speed a_b into the burned gas while being convected with velocity $-V$. Another cylindrical wave is generated at point P_1 at time t_1 and propagates into the combustible mixture with speed a_c. The cylindrical wave fronts thus generated form envelopes (Mach lines) in both the combustible mixture and the burned gas, which constitute plane sound waves.

For the wave-inclination angle φ shown in figure 1(b), an envelope cannot be formed on the burned-gas side of the flame front. The cylindrical sound waves thus expand independently and are thereby attenuated. On the combustible-mixture side of the front, the cylindrical sound waves meet at the common tangent point P_2. For inclination angles less than the critical angle shown, attenuating pressure waves are also produced in the combustible mixture until another critical angle $180°-\varphi$ is reached. Below this second critical angle, plane sound waves are again obtained. These critical angles may be obtained from the geometry of figure 1(b). For small flame Mach numbers where $M \equiv \frac{U}{a_c}$,

$$\varphi_{cr,c} = \sin^{-1} M$$

$$\varphi_{cr,b} = \sin^{-1} \frac{M}{\sqrt{\tau}}$$

As the flame Mach number M decreases, attenuating waves are produced for a wider range of inclination angle. In the limiting case of very slow flow (constant-pressure combustion),[2] only attenuating pressure waves appear in combination with the vorticity waves if $0°<\varphi<180°$. Quantities associated with the pressure wave vanish when $\varphi=0°$ or 180° because the incident vorticity wave then passes through the combustion front without distorting the front.

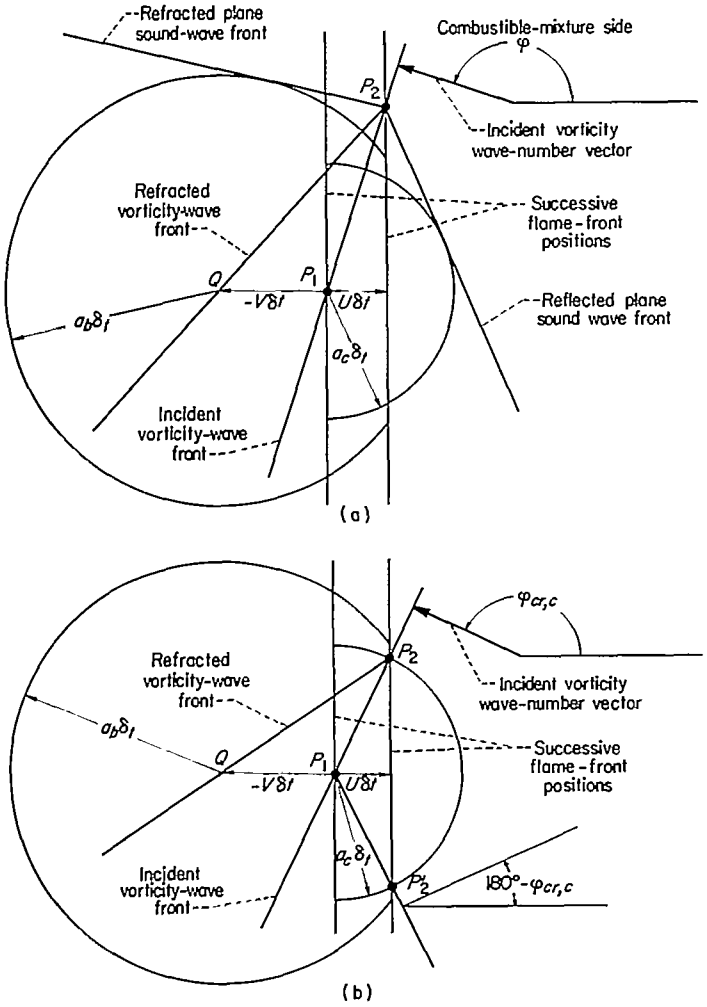

(a) Interaction for wave-number vector inclinations generating plane sound waves.

(b) Interaction for wave-number vector inclinations generating noncoalescing cylindrical sound waves.

FIGURE 1.—Wave formation arising from interaction of flame front with vorticity wave.

SINGLE-WAVE ANALYSIS

TWO-DIMENSIONAL FORMULATION

The interaction process described in the preceding section is now formulated analytically for the passage of a combustion front through a single weak two-dimensional vorticity wave of constant density inclined to the flame front. The case of a vorticity wave in three dimensions is considered later.

The combustion front is assumed to be completely specified by its laminar flame velocity U and the ratio of stagnation temperatures τ in the burned gas and in the combustible mixture, respectively. In the absence of any perturbations, the equations for conservation of momentum, energy, and mass-flow rate, respectively, as written for a reference frame moving with the flame front, are

$$\left.\begin{aligned} p_c+\rho_c U^2&=p_b+\rho_b(U-V)^2 \\ \tau\left(\frac{\gamma R_g}{\gamma-1}T_c+\frac{1}{2}U^2\right)&=\frac{\gamma R_g}{\gamma-1}T_b+\frac{1}{2}(U-V)^2 \\ \rho_c U&=\rho_b(U-V) \end{aligned}\right\} \quad (1)$$

where subscripts c and b designate stations in the combustible mixture and in the burned gas, respectively. For simplicity it has been assumed that the combustion process does not entail a change in the number of moles per unit mass of gas; also, differences in the ratio of specific heats for the burned and unburned gas are ignored. The quantity $(\tau-1)$ is then indicative of the increase in stagnation enthalpy or heat release.

For the interaction problem the resulting flame-front distortion $\xi'(y,t)$ must be considered in addition to the generated disturbances previously mentioned. Thus, both the flame-front perturbation velocity $\frac{\partial \xi'}{\partial t}\equiv\xi'_t$ and the instantaneous flame-front slope $\frac{\partial \xi'}{\partial y}\equiv\xi'_y$ will appear in the equations of motion. The conservation equations may still be applied in a coordinate system moving instantaneously with the distorted flame front since extreme gradients occur across the front and small disturbances are postulated. The various perturbation quantities (designated by primes) are assumed to have zero space or time averages. The flame speed U_T (see sketch (b)) will thus include any time-

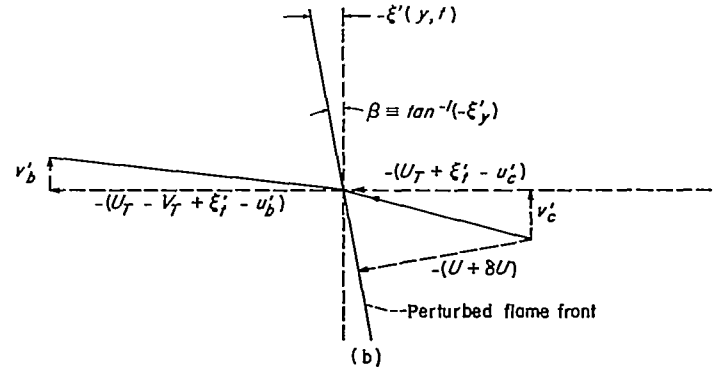

independent contributions arising from the perturbations. Conservation of normal and tangential momentum, energy, and mass-flow rate provides the following relations:

[2] It can be shown that the static-pressure ratio across a flame front is given by $p_b/p_c=1-\gamma(\tau-1)M^2+\ldots$.

$$(p_c+p_c')[1+(\xi_y')^2]+(\rho_c+\rho_c')[(U_T+\xi_t'-u_c')^2+(v_c')^2(\xi_y')^2+2(U_T+\xi_t'-u_c')v_c'\xi_y']$$
$$=(p_b+p_b')[1+(\xi_y')^2]+(\rho_b+\rho_b')[(U_T-V_T+\xi_t'-u_b')^2+(v_b')^2(\xi_y')^2+2(U_T-V_T+\xi_t'-u_b')v_b'\xi_y'] \tag{2a}$$

$$(U_T+\xi_t'-u_c')\xi_y'-v_c'=(U_T-V_T+\xi_t'-u_b')\xi_y'-v_b' \tag{2b}$$

$$(\tau+\tau')\left[\frac{\gamma R_g}{\gamma-1}(T_c+T_c')+\frac{1}{2}(U_T+\xi_t'-u_c')^2+\frac{1}{2}(v_c')^2\right]=\frac{\gamma R_g}{\gamma-1}(T_b+T_b')+\frac{1}{2}(U_T-V_T+\xi_t'-u_b')^2+\frac{1}{2}(v_b')^2 \tag{2c}$$

$$(\rho_c+\rho_c')(U_T+\xi_t'-u_c'+v_c'\xi_y')=(\rho_b+\rho_b')(U_T-V_T+\xi_t'-u_b'+v_b'\xi_y') \tag{2d}$$

Small-perturbation techniques are used to make the interaction problem amenable to analysis. Then, if the velocity perturbations are assumed to be small relative to the flame speed U_T and the flame-front slope ξ_y' is also assumed to be very small so that terms of the second order in the fluctuation quantities may be neglected, application of the linearized state equation $\frac{p'}{p}=\frac{\rho'}{\rho}+\frac{T'}{T}$ and utilization of equations (1) permit the following boundary conditions at the flame front to be obtained from equations (2):

$$\frac{p_b'}{p_b}+B_1\frac{\rho_b'}{\rho_b}+B_2\frac{\xi_t'-u_b'}{U}=B_3\frac{p_c'}{p_c}+B_2\frac{\xi_t'-u_c'}{U} \tag{3a}$$

$$\frac{v_b'}{U}=\frac{v_c'}{U}+E_1\xi_y' \tag{3b}$$

$$\frac{p_b'}{p_b}-\frac{\rho_b'}{\rho_b}+K_1\frac{\xi_t'-u_b'}{U}=K_2\frac{p_c'}{p_c}+K_3\tau'+K_4\frac{\xi_t'-u_c'}{U} \tag{3c}$$

$$\frac{\rho_b'}{\rho_b}+D_1\frac{\xi_t'-u_b'}{U}=\frac{\xi_t'-u_c'}{U}+\frac{1}{\gamma}\frac{p_c'}{p_c} \tag{3d}$$

where

$$\left.\begin{gathered}B_1\equiv\frac{\gamma U^2}{a_b^2}\left(\frac{U-V}{U}\right)^2,\ B_2\equiv\frac{2\gamma U^2}{a_b^2}\left(\frac{U-V}{U}\right),\ B_3\equiv\frac{U-V}{U}\left(\frac{U^2}{a_b^2}\right)\left(1+\frac{a_c^2}{U^2}\right),\ D_1\equiv\frac{U}{U-V},\ E_1\equiv\frac{-V}{U}\\ K_1\equiv(\gamma-1)\frac{U^2}{a_b^2}\left(\frac{U-V}{U}\right),\ K_2\equiv\frac{\gamma-1}{\gamma}\tau\frac{a_c^2}{a_b^2},\ K_3\equiv\left(\frac{c_pT_{S,c}}{U^2}\right)(\gamma-1)\frac{U^2}{a_b^2},\ K_4\equiv(\gamma-1)\tau\frac{U^2}{a_b^2}\\ a_c^2\equiv\gamma R_gT_c,\ a_b^2\equiv\gamma R_gT_b\end{gathered}\right\} \tag{4}$$

It has also been assumed that the flow upstream of the flame is isentropic. It will be shown in the section TURBULENT FLAME SPEED that $U_T=U$ is correct through first-order terms.

Another relation is required at the flame front. For the two-dimensional case under consideration, the local instantaneous normal propagation velocity $U+\delta U$ of the distorted flame front into the combustible mixture at rest (see sketch (b)) is

$$U+\delta U=\frac{U_T+\xi_t'-u_c'+v_c'\xi_y'}{\sqrt{1+(\xi_y')^2}}$$

The incremental propagation velocity δU will be determined from existing information on laminar flames. Some support for this procedure is given in reference 13. As reported therein, radiant flux-intensity measurements on laminar and turbulent propane-air flames suggest that a small surface element of a turbulent flame is chemically and physically the same as that of a corresponding laminar flame.

The propagation speed of a laminar flame is affected by both the ambient pressure and temperature. Although the functional relations have not been rigorously determined, preliminary indications are that the pressure effect is much smaller than the temperature effect. In the present analysis the local flame-propagation speed is assumed to depend only upon the temperature of the combustible mixture, that is,

$$\delta U=\frac{dU}{dT_c}dT_c=\left(\frac{dU}{dT_c}\right)T_c'$$

With the empirical relation obtained in reference 14 as a guide, it is assumed that $U=r_1+r_2T_c^n$ where r_1, r_2, and n are constants which depend upon the fuel and oxidant under consideration. Thus,

$$\delta U=nr_2T_c^n\left(\frac{T_c'}{T_c}\right)=nr_2\left(\frac{\gamma-1}{\gamma}\right)T_c^n\left(\frac{p_c'}{p_c}\right)\equiv U\Lambda\frac{p_c'}{p_c}$$

and

$$U\left(1+\Lambda\frac{p_c'}{p_c}\right)\sqrt{1+\xi_y'^2}=U_T+\xi_t'-u_c'+v_c'\xi_y'$$

Correct through first-order terms wherein $U_T=U$, the following boundary condition is obtained at the flame front:

$$\frac{\xi_t'-u_c'}{U}=\Lambda\frac{p_c'}{p_c} \tag{3e}$$

In a coordinate system fixed in space, the equations of motion for the two-dimensional fluctuation quantities in

the burned gas with terms of the second order neglected are

$$\frac{\partial u_b'}{\partial t}+V\frac{\partial u_b'}{\partial x_c}=-\frac{1}{\rho_b}\frac{\partial p_b'}{\partial x_c}$$

$$\frac{\partial v_b'}{\partial t}+V\frac{\partial v_b'}{\partial x_c}=-\frac{1}{\rho_b}\frac{\partial p_b'}{\partial y}$$

$$\frac{\partial \rho_b'}{\partial t}+V\frac{\partial \rho_b'}{\partial x_c}+\rho_b\left(\frac{\partial u_b'}{\partial x_c}+\frac{\partial v_b'}{\partial y}\right)=0$$

$$\rho_b c_v\frac{\partial T_b'}{\partial t}+\rho_b c_v V\frac{\partial T_b'}{\mathrm{d}x_c}+p_b\left(\frac{\partial u_b'}{\partial x_c}+\frac{\partial v_b'}{\mathrm{d}y}\right)=0$$

For a coordinate system moving with constant velocity V, the preceding equations reduce to the same form as the corresponding equations for the fluctuation quantities in the combustible mixture relative to a coordinate system fixed in space. Thus, the flow equations for both the combustible-mixture fluctuations and the burned-gas fluctuations may be written, with appropriate subscripts c or b, as

$$\left.\begin{aligned}\frac{\partial u'}{\partial t}&=-\frac{1}{\rho}\frac{\partial p'}{\partial x}\\ \frac{\partial v'}{\partial t}&=-\frac{1}{\rho}\frac{\partial p'}{\partial y}\\ \frac{\partial \rho'}{\partial t}&=-\rho\left(\frac{\partial u'}{\partial x}+\frac{\partial v'}{\partial y}\right)\\ \rho c_v\frac{\partial T'}{\partial t}&=-\rho\left(\frac{\partial u'}{\partial x}+\frac{\partial v'}{\partial y}\right)\end{aligned}\right\} \tag{5}$$

The coordinate systems x_c,y and x_b,y for the first-order analysis are indicated in sketch (c).

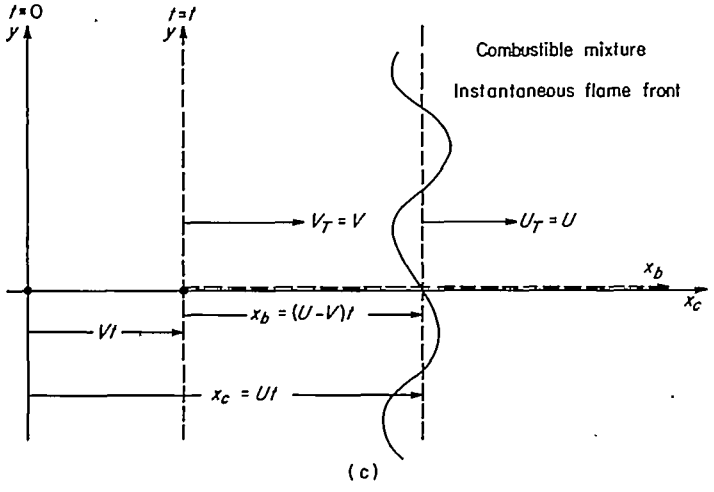

(c)

A two-dimensional vorticity wave in the combustible mixture with velocity vector of magnitude A that has its wave-number vector $\underline{k}$ inclined at an angle φ to the positive direction of the x_c-axis may be written in the form

$$\frac{u_{s,c}'}{U}=(A\sin\varphi)e^{i\nu},\ \frac{v_{s,c}'}{U}=(-A\cos\varphi)e^{i\nu}$$

where $\nu\equiv k_1'x_c+k_2'y$, and k_1' and k_2' are components of the wave-number vector $\underline{k}$ in the x_c- and y-directions, respectively, with $k_2'/k_1'=\tan\varphi$. As a result of the linear boundary conditions of equations (3), obtaining a unique solution of the interaction problem requires that the arguments of all disturbance waves match at the flame front. This matching requirement together with provision for differences in phase angle yields the following form for the vorticity wave present in the burned gas:

$$\frac{u_{s,b}'}{U}=(G_1+iG_2)e^{i\psi},\ \frac{v_{s,b}'}{U}=(I_1+iI_2)e^{i\psi}$$

where

$$\psi\equiv\left(\frac{U}{U-V}\right)k_1'x_b+k_2'y$$

Pressure fluctuations generated by the interaction must satisfy the following wave equation, with appropriate subscripts c or b, which is obtainable from equations (5):

$$\frac{\partial^2 p'}{\partial t^2}-a^2\left(\frac{\partial^2 p'}{\partial x^2}+\frac{\partial^2 p'}{\partial y^2}\right)=0 \tag{6}$$

The present analysis will be concerned with the limiting case of very slow flow (constant-pressure combustion). It is clear from the relations given for the critical wave-inclination angles $\varphi_{cr,c}$ and $\varphi_{cr,b}$ that, for very slow flows, only the irrotational isentropic pressure waves described in the section FLAME-TURBULENCE INTERACTION PROCESS will be generated by the interaction. The form of these pressure waves that satisfies equation (6) has already been established in reference 12 in terms of the variables η and ζ, where

$$\left.\begin{aligned}\eta_c&\equiv(f_c)(x_c-Ut)\\ \zeta_c&\equiv b_c x_c+c_c y+Ud_c t\\ \eta_b&\equiv(f_b)[-x_b+(U-V)t]\\ \zeta_b&\equiv b_b x_b+c_b y+Ud_b t\end{aligned}\right\} \tag{7}$$

The variable η is proportional to the distance from the flame front. At the front, $\eta_c=\eta_b=0$; upstream of the flame, η_c is positive; and downstream of the flame, η_b is positive. The equation ζ=constant defines planes moving with constant velocity $(Ud)_{c,b}$ at an angle $\tan^{-1}(c/b)_{c,b}$ to the flame velocity U. Equation (6) takes the form of the Laplace equation

$$\left(\frac{\partial^2}{\partial\eta^2}+\frac{\partial^2}{\partial\zeta^2}\right)\frac{p'}{p}=0$$

when

$$\left.\begin{aligned}\left(\frac{\partial\eta}{\partial t}\right)^2-\left(\frac{\partial\zeta}{\partial t}\right)^2&=a^2\left[\left(\frac{\partial\eta}{\partial x}\right)^2-\left(\frac{\partial\zeta}{\partial x}\right)^2-\left(\frac{\partial\zeta}{\partial y}\right)^2\right]\\ \frac{\partial\eta}{\partial t}\frac{\partial\zeta}{\partial t}&=a^2\frac{\partial\eta}{\partial x}\frac{\partial\zeta}{\partial x}\end{aligned}\right\} \tag{8}$$

Matching arguments of the pressure and vorticity waves at the combustion front where $\eta=0$ and satisfying the require-

ments of equations (8) provide the following values for the constants of equations (7):

$$\left.\begin{aligned} c_c=c_b=k_2',\ b_c=-\frac{k_1'M^2}{1-M^2},\ b_b=\frac{-k_1'\left(\frac{U-V}{U}\right)\frac{U^2}{a_b^2}}{1-\left(\frac{U-V}{U}\right)^2\frac{U^2}{a_b^2}},\ d_c=\frac{k_1'}{1-M^2} \\ d_b=\frac{k_1'}{1-\left(\frac{U-V}{U}\right)^2\frac{U^2}{a_b^2}},\ f_c^2=\frac{b_c^2+c_c^2-d_c^2M^2}{1-M^2},\ f_b^2=\frac{b_b^2+c_b^2-d_b^2\frac{U^2}{a_b^2}}{1-\left(\frac{U-V}{U}\right)^2\frac{U^2}{a_b^2}} \end{aligned}\right\} \tag{9}$$

In addition to the boundary condition from equations (3), the pressure fluctuations will be required to satisfy the boundary condition $\frac{p'}{p}=0$ at $\eta=\infty$. Utilizing equations (36) and (37) of reference 12 yields

$$\frac{p_c'}{p_c}=(R_1+iR_2)e^{i\zeta_c-\eta_c} \tag{10a}$$

$$\frac{p_b'}{p_b}=(J_1+iJ_2)e^{i\zeta_b-\eta_b} \tag{10b}$$

In the combustible mixture, density fluctuations are associated only with the pressure fluctuations according to the isentropic relation $\frac{\rho_c'}{\rho_c}=\frac{1}{\gamma}\frac{p_c'}{p_c}$. In the burned gas, density fluctuations may also be caused by entropy fluctuations generated by flame distortion and heat-release fluctuations, if present, as well as by pressure fluctuations. Velocity fluctuations are associated with both pressure fluctuations and vorticity fluctuations. It is convenient to deal with the pressure coefficient p'/ρ_cU_2. Thus, the disturbances arising from the interaction of the flame front and incident vorticity wave take the following forms:

$$\frac{p_c'}{\rho_cU^2}=\frac{1}{\gamma M^2}(R_1+iR_2)e^{i\zeta_c-\eta_c}\equiv(R^{(1)}+iR^{(2)})e^{i\zeta_c-\eta_c} \tag{10c}$$

$$\frac{p_b'}{\rho_cU^2}=\frac{p_b}{\rho_cU^2}(J_1+iJ_2)e^{i\zeta_b-\eta_b}\equiv(J^{(1)}+iJ^{(2)})e^{i\zeta_b-\eta_b} \tag{10d}$$

$$\frac{\rho_b'}{\rho_b}=\frac{1}{\gamma}(J_1+iJ_2)e^{i\zeta_b-\eta_b}+(L_1+iL_2)e^{i\psi} \tag{10e}$$

$$\frac{u_b'}{U}=(N_1+iN_2)e^{i\zeta_b-\eta_b}+(G_1+iG_2)e^{i\psi} \tag{10f}$$

$$\frac{v_b'}{U}=(P_1+iP_2)e^{i\zeta_b-\eta_b}+(I_1+iI_2)e^{i\psi} \tag{10g}$$

$$\frac{u_c'}{U}=(W_1+iW_2)e^{i\zeta_c-\eta_c}+(A\sin\varphi)e^{i\nu} \tag{10h}$$

$$\frac{v_c'}{U}=(X_1+iX_2)e^{i\zeta_c-\eta_c}-(A\cos\varphi)e^{i\nu} \tag{10i}$$

The flame displacement velocity may be written

$$\frac{\xi_t'}{U}=(H_1+iH_2)e^{i(k_1'Ut+k_2'y)}\equiv(H_1+iH_2)e^{i\sigma} \tag{10j}$$

To satisfy the requirements that the arguments of all disturbance quantities match at the flame front and that $\frac{\partial^2\xi}{\partial t\partial y}=\frac{\partial^2\xi}{\partial y\partial t}$, the flame-front slope must take the form

$$\xi_y'=(H_1+iH_2)(\tan\varphi)e^{i\sigma} \tag{10k}$$

Integration of equation (10j) with respect to time t gives the flame displacement as

$$\xi'=\frac{1}{k_1'}(H_2-iH_1)e^{i\sigma}=\frac{\tan\varphi}{k_2'}(H_2-iH_1)e^{i\sigma} \tag{10l}$$

EXTENSION TO THREE-DIMENSIONAL DISTURBANCES

Equations (10) describe the interaction of a flame front with a constant-density vorticity wave having velocity components

$$\frac{u_{s,c}'}{U}=(A\sin\varphi)e^{i\nu}\text{ and }\frac{v_{s,c}'}{U}=(-A\cos\varphi)e^{i\nu}$$

in the x_c- and y-directions, respectively. The vorticity wave may be considered to have a third velocity component $\frac{w_{s,c}'}{U}=Ce^{i\nu}$ in the z-direction. In the preceding linearized analysis, the amplitude C was not prescribed. This component, which is normal to both the u' and v' components and parallel to the plane of the flame front, then is associated with a corresponding component of the vorticity wave in the burned gas $\frac{w_{s,b}'}{U}=Ce^{i\psi}$.

Inasmuch as turbulence fields are three-dimensional, the interaction equations must be revised accordingly for application to the spectral analysis which follows. Assume, as shown in sketch (d), that the polarization plane which will contain the wave-number vector $\underline{k}$ is inclined at some angle θ to the $x_{1,c}x_{2,c}$-plane of a new coordinate system $x_{1,c}$, $x_{2,c}$, $x_{3,c}$ fixed in space for the combustible mixture.

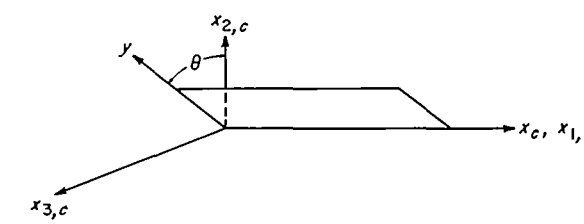

(d)

The corresponding coordinate system $x_{1,b}$, $x_{2,b}$, $x_{3,b}$ for the burned gas is assumed to be moving with mean flow velocity V. Components k_1, k_2, and k_3 of the wave-number vector k in the directions of $x_{1,c}$, $x_{2,c}$, and $x_{3,c}$, respectively, are

$$\left.\begin{aligned} k_1&=k\cos\varphi \\ k_2&=k\sin\varphi\cos\theta \\ k_3&=k\sin\varphi\sin\theta \end{aligned}\right\} \tag{11}$$

With primed perturbation vector quantities referring to the original coordinates x_c, x_b, y, z and unprimed perturbation vector quantities referring to the $x_{1,c}$, $x_{2,c}$, $x_{3,c}$- and $x_{1,b}$, $x_{2,b}$,

$x_{3,b}$-coordinate systems, the following transformation relations apply:

$$\left.\begin{aligned} u_{1,c}&=u'_c \qquad u_{1,b}=u'_b \\ u_{2,c}&=v'_c\cos\theta-w'_c\sin\theta \qquad u_{2,b}=v'_b\cos\theta-w'_b\sin\theta \\ u_{3,c}&=v'_c\sin\theta+w'_c\cos\theta \qquad u_{3,b}=v'_b\sin\theta+w'_b\cos\theta \\ \xi&=\xi' \\ \xi_t&=\xi'_t \\ \xi_{x_{2,c}}&=\xi'_y\cos\theta \\ \xi_{x_{3,c}}&=\xi'_y\sin\theta \end{aligned}\right\} \quad (12)$$

This notation refers only to equations (12).

With the use of equations (10) and (12), the interaction fluctuation quantities (again designated by primes) referred to the coordinate axes $x_{1,c}$, $x_{2,c}$, $x_{3,c}$ and $x_{1,b}$, $x_{2,b}$, $x_{3,b}$ may be written as

$$\left.\begin{aligned} \frac{p'_c}{\rho_c U^2}&=(R^{(1)}+iR^{(2)})e^{i\tau_c-\eta_c} \\ \frac{p'_b}{\rho_c U^2}&=(J^{(1)}+iJ^{(2)})e^{i\tau_b-\eta_b} \\ \frac{\rho'_c}{\rho_c}&=\frac{1}{\gamma}(R_1+iR_2)e^{i\tau_c-\eta_c} \\ \frac{\rho_b}{\rho_b}&=\frac{1}{\gamma}(J_1+iJ_2)e^{i\tau_b-\eta_b}+(L_1+iL_2)e^{i\psi} \\ \frac{u'_{1,c}}{U}&=(W_1+iW_2)e^{i\tau_c-\eta_c}+(A\sin\varphi)e^{i\nu} \\ \frac{u'_{2,c}}{U}&=(X_1+iX_2)(\cos\theta)e^{i\tau_c-\eta_c}-(A\cos\varphi\cos\theta+C\sin\theta)e^{i\nu} \\ \frac{u'_{3,c}}{U}&=(X_1+iX_2)(\sin\theta)e^{i\tau_c-\eta_c}-(A\cos\varphi\sin\theta-C\cos\theta)e^{i\nu} \\ \frac{u'_{1,b}}{U}&=(N_1+iN_2)e^{i\tau_b-\eta_b}+(G_1+iG_2)e^{i\psi} \\ \frac{u'_{2,b}}{U}&=(P_1+iP_2)(\cos\theta)e^{i\tau_b-\eta_b}+[(I_1+iI_2)\cos\theta-C\sin\theta]e^{i\psi} \\ \frac{u'_{3,b}}{U}&=(P_1+iP_2)(\sin\theta)e^{i\tau_b-\eta_b}+[(I_1+iI_2)\sin\theta+C\cos\theta]e^{i\psi} \\ \frac{\xi'_t}{U}&=(H_1+iH_2)e^{i\sigma} \\ \xi'_{x_{2,c}}&=(H_1+iH_2)(\tan\varphi\cos\theta)e^{i\sigma} \\ \xi'_{x_{3,c}}&=(H_1+iH_2)(\tan\varphi\sin\theta)e^{i\sigma} \\ \xi'&=\frac{(H_2-iH_1)e^{i\sigma}}{k'_1} \end{aligned}\right\} \quad (13)$$

The fluctuation amplitude coefficients of equation (10) or (13) may be determined from equations (3) and (5). Details of the solution are given in appendixes B and C. The general solution for the attenuating pressure-wave regime is indicated in appendix B. Inasmuch as the flame Mach number $M\equiv\frac{U}{a_c}$ is generally much less than 0.01, the limiting case of very slow flow (constant-pressure combustion) provides a reasonable simplification of the problem and only the attenuating-wave solution need be considered. The amplitude coefficients for this limiting case are given in appendix C (eqs. (C8)).

Equations (13) and (C8) describe the linearized interaction of a constant-pressure flame front with a single vorticity wave or shear wave having its wave-number vector $\underline{k}$ inclined at an angle φ to the direction of travel of the undisturbed flame front and having its plane of polarization inclined at an angle θ to the $x_{1,c}$, $x_{2,c}$-plane of the coordinate axes $x_{1,c}$, $x_{2,c}$, $x_{3,c}$. The wave-number vector of the shear wave generated in the burned gas makes an angle $\varphi_b=\tan^{-1}(\tau\tan\varphi)$ with the direction of propagation of the undisturbed flame front. Attenuating potential fields are generated in both the combustible mixture and the burned gas. Physical quantities associated with these fields attenuate exponentially with increasing distance from the flame front. The amplitude coefficients for a given heat release (a prescribed τ) and a given inclination angle φ and a polarization angle θ depend upon both the intensity of the incident vorticity wave and the heat-release perturbation parameter τ'/τ. In the absence of such heat-release perturbations, there are no density fluctuations in the burned gas (correct to order M^2).

These single-wave results may be used to determine the interaction of a constant-pressure combustion front with a turbulence field of constant density for the case of negligible turbulence decay. The turbulence field will contain an infinite number of transverse plane waves with all wavelengths and planes of polarization. The spectral analysis technique used in obtaining such a superposition of waves will be discussed briefly before proceeding with the interaction problem.

SPECTRAL ANALYSIS

GENERAL CONSIDERATIONS

A turbulence field satisfying the incompressible-flow continuity equation may be represented by the following superposition of plane transverse waves:

$$\underline{u}(\underline{x},t)\iiint_{-\infty}^{\infty} e^{i\underline{k}\cdot\underline{x}}\,d\underline{Z}(\underline{k},t)$$

where $\underline{x}$ is a position vector, $\underline{k}$ is a wave-number vector, t is the time, and $d\underline{Z}(\underline{k},t)$ is the random amplitude vector of a component wave. The quantity $d\underline{Z}(\underline{k},t)e^{i\underline{k}\cdot\underline{x}}$ represents the contribution to the velocity field from a volume element $d\underline{k}$ in wave-number space. When, as in the present case, the equations of motion are linear there is no modulation or interference between component waves, and the various statistical quantities describing a random field may be obtained from the results of a single-wave analysis. To avoid the interpretative difficulties associated with the random variable $\underline{Z}(\underline{k},t)$, which is nondifferentiable with respect to $\underline{k}$, use is made of the techniques of references 10 and 15, which utilize correlation spectra rather than amplitude spectra in the analysis of homogeneous turbulence.

A velocity correlation is defined as the ensemble average $\overline{u_i(\underline{x},t)u_j(\underline{x}',t)}$ of the product of a fluctuation-velocity component u_i at $\underline{x}$ and a component u_j at $\underline{x}'=\underline{x}+\underline{r}$ where $\underline{r}$ is a separation vector. The subscripts i and j take on the values 1, 2, and 3. The ensemble average, designated by a bar, may be regarded as the result of averaging the product $u_i(\underline{x},t)u_j(\underline{x},t)$ at a given instant over a very large number of statistically similar fields. The nine velocity correlations u_iu_j constitute the velocity correlation tensor $T_{ij}(\underline{x},\underline{x}',t)$. For a homogeneous field, T_{ij} depends only on $\underline{r}$ so that the tensor may be written $T_{ij}(\underline{r},t)$.

As shown in references 10 and 15, the velocity correlation tensor has the following Fourier integral expansion:

$$T_{ij}(\underline{r},t)=\iiint_{-\infty}^{\infty} e^{i(\underline{k}\cdot\underline{r})}\,dF_{ij}(\underline{k},t)=\iiint_{-\infty}^{\infty} e^{i(\underline{k}\cdot\underline{r})}\Phi_{ij}(\underline{k},t)d\underline{k} \qquad (14)$$

where $F_{ij}(\underline{k},t)$ is the spectral tensor function, $\Phi_{ij}(\underline{k},t)$ is the spectral tensor density of a homogeneous turbulence field, and

$$\Phi_{ij}(\underline{k},t)d\underline{k}=\overline{dZ_i^*(\underline{k},t)dZ_j(\underline{k},t)} \qquad (15)$$

where $dZ_i^*(\underline{k},t)$ denotes the complex conjugate of $dZ_i(\underline{k},t)$. For $r=0$ and $i=j$, equation (14) may be written

$$T_{ii}(0,t)=\overline{u_i^2}=\iiint_{-\infty}^{\infty}\overline{dZ_i^*(\underline{k},t)dZ_i(\underline{k},t)} \qquad (16)$$

For homogeneous turbulence fields, wherein ensemble averages and space averages are identical, equations (15) and (16) provide the basis for obtaining the spatial mean-square velocity components from the single-wave results given by equations (13) and (C8). Equations (15) and (16) are also applicable to scalar fields. In the absence of viscosity, as postulated, the shear-velocity fields present in the combustible mixture and in the burned gas are homogeneous, and application of equation (16) presents no complications. The corresponding potential-flow fields, although spatially inhomogeneous, are homogeneous in the given x_2,x_3-planes. It has been shown in reference 16 that equation (16), in effect, may be applied for such fields to obtain the mean-square fluctuations pertaining to a given plane of homogeneity.

As a result of the preceding discussion, the single-wave interaction results for constant-pressure combustion will be used to obtain the spectral densities of the fluctuation quantities at the flame front where the attenuation factors $e^{-\nu_c}$ and $e^{-\nu_b}$ are unity and $\zeta_c=\zeta_b=\sigma=\psi=\nu$. For conciseness, define $RA\sin\varphi\equiv R^{(1)}+iR^{(2)}$, $WA\sin\varphi\equiv W_1+iW_2$, $GA\sin\varphi\equiv G_1+iG_2$, $NA\sin\varphi\equiv N_1+iN_2$, $HA\sin\varphi\equiv H_1+iH_2$, and $C^1A\sin\varphi\equiv C$. With the notation

$$\overline{u_{1,s,c}^2}\equiv\iiint_{-\infty}^{\infty}\overline{dZ_{1,c}^*\,dZ_{1,c}}$$

and, for example,

$$\overline{\left(\frac{p_c'}{\rho_cU^2}\right)^2}\equiv\iiint_{-\infty}^{\infty}\overline{d\left(\frac{p_c'}{\rho_cU^2}\right)^*\,d\left(\frac{p_c'}{\rho_cU^2}\right)}$$

as in equation (16), the following equations are obtained by analogy with equations (13) and (C8) for the case where heat-release perturbations are absent, that is, $\tau'=0$:

$$\left.\begin{aligned}
d\left(\frac{p_c'}{\rho_cU^2}\right)&=d\left(\frac{p_b'}{\rho_cU^2}\right)=R\,dZ_{1,c}\\
d\left(\frac{u_{1,c}'}{U}\right)&=W\,dZ_{1,c}+dZ_{1,c}\\
d\left(\frac{u_{2,c}'}{U}\right)&=-iW\cos\theta\,dZ_{1,c}-(\cot\varphi\cos\theta+C^1\sin\theta)dZ_{1,c}\\
d\left(\frac{u_{3,c}'}{U}\right)&=-iW\sin\theta\,dZ_{1,c}-(\cot\varphi\sin\theta-C^1\cos\theta)dZ_{1,c}\\
d\left(\frac{u_{1,b}}{U}\right)&=N\,dZ_{1,c}+G\,dZ_{1,c}\\
d\left(\frac{u_{2,b}'}{U}\right)&=iN\cos\theta\,dZ_{1,c}-\left(\frac{\cot\varphi\cos\theta}{\tau}G+C^1\sin\theta\right)dZ_{1,c}\\
d\left(\frac{u_{3,b}'}{U}\right)&=iN\sin\theta\,dZ_{1,c}-\left(\frac{\cot\varphi\sin\theta}{\tau}G-C^1\cos\theta\right)dZ_{1,c}\\
d(\xi')&=-\frac{iH}{k_1'}dZ_{1,c}=-\frac{iH}{k\cos\varphi}dZ_{1,c}\\
d\left(\frac{\xi_t}{U}\right)&=H\,dZ_{1,c}\\
d(\xi'_{x_2,c})&=H\tan\varphi\cos\theta\,dZ_{1,c}\\
d(\xi'_{x_3,c})&=H\tan\varphi\sin\theta\,dZ_{1,c}
\end{aligned}\right\} \qquad (17)$$

In the velocity ratios of equations (17), the first term on the right side represents the potential-flow contributions $\frac{u_{i,p,c}}{U}$ or $\frac{u_{i,p,b}}{U}$; the second term represents the shear-flow contributions $\frac{u_{i,s,c}}{U}$ or $\frac{u_{i,s,b}}{U}$. The subscript i takes on the values 1, 2, and 3.

At a given instant the spatial mean-square potential- and shear-flow contributions of the disturbance fields are obtained from equations (17):

$$\left.\begin{aligned}
\overline{\left(\frac{p'_c}{\rho_c U^2}\right)^2}=\overline{\left(\frac{p'_b}{\rho_c U^2}\right)^2}&=\int_{-\infty}^{\infty}\int\int (R^*R)\,\overline{dZ^*_{1,c}\,dZ_{1,c}}\\
\overline{\left(\frac{u_{1,s,c}}{U}\right)^2}&=\int_{-\infty}^{\infty}\int\int \overline{dZ^*_{1,c}\,dZ_{1,c}}\\
\overline{\left(\frac{u_{2,s,c}}{U}\right)^2}+\overline{\left(\frac{u_{3,s,c}}{U}\right)^2}&=\int_{-\infty}^{\infty}\int\int \overline{dZ^*_{2,c}\,dZ_{2,c}}+\overline{dZ^*_{3,c}\,dZ_{3,c}}\\
\overline{\left(\frac{u_{1,p,c}}{U}\right)^2}=\overline{\left(\frac{u_{2,p,c}}{U}\right)^2}+\overline{\left(\frac{u_{3,p,c}}{U}\right)^2}&=\int_{-\infty}^{\infty}\int\int (W^*W)\,\overline{dZ^*_{1,c}\,dZ_{1,c}}\\
\overline{\left(\frac{u_{1,s,b}}{U}\right)^2}&=\int_{-\infty}^{\infty}\int\int (G^*G)\,\overline{dZ^*_{1,c}\,dZ_{1,c}}\\
\overline{\left(\frac{u_{2,s,b}}{U}\right)^2}+\overline{\left(\frac{u_{3,s,b}}{U}\right)^2}=\overline{\left(\frac{u_{2,s,c}}{U}\right)^2}+\overline{\left(\frac{u_{3,s,c}}{U}\right)^2}&+\int_{-\infty}^{\infty}\int\int \left(\frac{\cot\varphi}{\tau}\right)^2 (G^*G-\tau)^2\,\overline{dZ^*_{1,c}\,dZ_{1,c}}\\
\overline{\left(\frac{u_{1,p,b}}{U}\right)^2}=\overline{\left(\frac{u_{2,p,b}}{U}\right)^2}+\overline{\left(\frac{u_{3,p,b}}{U}\right)^2}&=\int_{-\infty}^{\infty}\int\int (N^*N)\,\overline{dZ^*_{1,c}\,dZ_{1,c}}
\end{aligned}\right\} \qquad (18)$$

The mean-square flame-front quantities are

$$\overline{\left(\frac{\xi_t}{U}\right)^2}=\int_{-\infty}^{\infty}\int\int (H^*H)\,\overline{dZ^*_{1,c}\,dZ_{1,c}}$$

$$\overline{\xi^2}=\int_{-\infty}^{\infty}\int\int \frac{(H^*H)}{k^2\cos^2\varphi}\,\overline{dZ^*_{1,c}\,dZ_{1,c}}$$

$$\overline{\xi^2_{x_{2,c}}}+\overline{\xi^2_{x_{3,c}}}=\int_{-\infty}^{\infty}\int\int (H^*H)\tan^2\varphi\,\overline{dZ^*_{1,c}\,dZ_{1,c}}$$

From equations (C8) of appendix C with $\tau'=0$:

$$\left.\begin{aligned}
R^*R&=\frac{(\tau-1)^2(\tau\tan^2\varphi-1)^2}{\Delta\sin^2\varphi}\\
W^*W&=\frac{(\tau-1)^2(\tau\tan^2\varphi-1)^2}{\Delta}\\
G^*G&=\frac{\tau^2\sec^2\varphi\,[\Delta-4\tau(\tau^2-1)\tan^2\varphi]}{\Delta(1+\tau^2\tan^2\varphi)}\\
N^*N&=\frac{\tau^2(\tau-1)^2(\tau\tan^2\varphi-1)^2\sec^2\varphi}{\Delta(1+\tau^2\tan^2\varphi)}\\
H^*H&=\frac{4\tau^2\sec^2\varphi}{\Delta}
\end{aligned}\right\} \qquad (19)$$

MEAN-SQUARE FLUCTUATIONS FOR INITIAL ISOTROPIC TURBULENCE

For a given combustion process (τ and U prescribed), the spatial mean-square fluctuations of equations (18) depend upon the quantity $\overline{dZ^*_{1,c}\,dZ_{1,c}}$, which is specified by the type of turbulence present in the combustible mixture. The results obtained in reference 16 for the interaction of axisymmetric turbulence with a shock wave suggest that for the present problem, the degree of anisotropy of the incident turbulence field may not be critical. For simplicity, the turbulence in the combustible mixture is assumed isotropic.

As indicated in reference 10, the spectral density tensors for any isotropic turbulence field satisfying the incompressible-flow continuity equation are

$$\Phi_{ij}(k)=\Omega(k)(k^2\delta_{ij}-k_ik_j) \qquad (20)$$

where $k^2=k_1^2+k_2^2+k_3^2$; $\delta_{ij}=1$ for $i=j$; $\delta_{ij}=0$ for $i\neq j$; and $\Omega(k)$ is the scalar amplitude function defining the spectral density tensor. From equations (15), (20), and (11),

$$\overline{dZ^*_{1,c}\,dZ_{1,c}}=\Omega(k)k^2\sin^2\varphi\,dk$$

or, transforming to spherical polar coordinates k, θ, φ, wherein $d\underline{k} \equiv dk_1\, dk_2\, dk_3 = k^2 \sin\varphi\, dk\, d\theta\, d\varphi$, yields

$$\left.\begin{aligned}
\overline{dZ^*_{1,c}\, dZ_{1,c}} &= \Omega(k)k^4\, dk\, d\theta \sin^3\varphi\, d\varphi \\
\overline{dZ^*_{2,c}\, dZ_{2,c}} &= \Omega(k)k^4\, dk\, d\theta \sin\varphi[\cos^2\varphi + \sin^2\varphi \sin^2\theta]d\varphi \\
\overline{dZ^*_{3,c}\, dZ_{3,c}} &= \Omega(k)k^4\, dk\, d\theta \sin\varphi[\cos^2\varphi + \sin^2\varphi \cos^2\theta]d\varphi \\
\overline{dZ^*_{2,c}\, dZ_{2,c}} + \overline{dZ^*_{3,c}\, dZ_{3,c}} &= \Omega(k)k^4\, dk\, d\theta \sin\varphi[1+\cos^2\varphi]d\varphi
\end{aligned}\right\} \quad (21)$$

The mean-square velocity components of the incident isotropic turbulence field are then given by

$$\left.\begin{aligned}
\overline{\left(\frac{u_{1,s,c}}{U}\right)^2} &= \int_0^\infty \Omega(k)k^4\, dk \int_0^{2\pi} d\theta \int_0^\pi \sin^3\varphi\, d\varphi = \frac{8\pi}{3}\int_0^\infty \Omega(k)k^4\, dk \\
\overline{\left(\frac{u_{2,s,c}}{U}\right)^2} + \overline{\left(\frac{u_{3,s,c}}{U}\right)^2} &= \int_0^\infty \Omega(k)k^4\, dk \int_0^{2\pi} d\theta \int_0^\pi \sin\varphi(1+\cos^2\varphi)d\varphi \\
&= \frac{16\pi}{3}\int_0^\infty \Omega(k)k^4\, dk
\end{aligned}\right\} \quad (22)$$

The remaining spatial mean-square fluctuation quantities, referred to the intensities of equations (22) in order that the scale need not be specified, are given by

$$\frac{\overline{\left(\frac{p'_c}{\rho_c U^2}\right)^2}}{\overline{\left(\frac{u_{1,s,c}}{U}\right)^2}} = \frac{\overline{\left(\frac{p'_b}{\rho_c U^2}\right)^2}}{\overline{\left(\frac{u_{1,s,c}}{U}\right)^2}} = \frac{3}{4}(\tau-1)^2 \int_0^\pi \frac{\sin\varphi}{\Delta}(\tau\tan^2\varphi - 1)^2 d\varphi \quad (23a)$$

$$\frac{\overline{\left(\frac{u_{1,p,c}}{U}\right)^2}}{\overline{\left(\frac{u_{1,s,c}}{U}\right)^2}} = \frac{\overline{\left(\frac{u_{2,p,c}}{U}\right)^2} + \overline{\left(\frac{u_{3,p,c}}{U}\right)^2}}{\overline{\left(\frac{u_{1,s,c}}{U}\right)^2}} = \frac{3}{4}(\tau-1)^2 \int_0^\pi \frac{\sin^3\varphi}{\Delta}(\tau\tan^2\varphi - 1)^2 d\varphi \quad (23b)$$

$$\frac{\overline{\left(\frac{u_{1,s,b}}{U}\right)^2}}{\overline{\left(\frac{u_{1,s,c}}{U}\right)^2}} = \frac{3\tau^2}{4}\int_0^\pi \frac{[\Delta - 4\tau(\tau^2-1)\tan^2\varphi]\sin\varphi\tan^2\varphi}{\Delta(1+\tau^2\tan^2\varphi)} d\varphi \quad (23c)$$

$$\frac{\overline{\left(\frac{u_{2,s,b}}{U}\right)^2} + \overline{\left(\frac{u_{3,s,b}}{U}\right)^2}}{\overline{\left(\frac{u_{2,s,c}}{U}\right)^2} + \overline{\left(\frac{u_{3,s,c}}{U}\right)^2}} = 1 - \frac{3}{8}(\tau^2-1)\int_0^\pi \frac{(\Delta + 4\tau\sec^2\varphi)\sin^3\varphi}{\Delta(1+\tau^2\tan^2\varphi)} d\varphi \quad (23d)$$

$$\frac{\overline{\left(\frac{u_{1,p,b}}{U}\right)^2}}{\overline{\left(\frac{u_{1,s,c}}{U}\right)^2}} = \frac{\overline{\left(\frac{u_{2,p,b}}{U}\right)^2} + \overline{\left(\frac{u_{3,p,b}}{U}\right)^2}}{\overline{\left(\frac{u_{1,s,c}}{U}\right)^2}}$$

$$= \frac{3}{4}\tau^2(\tau-1)^2 \int_0^\pi \frac{(\tau\tan^2\varphi - 1)^2 \sin\varphi\tan^2\varphi}{\Delta(1+\tau^2\tan^2\varphi)} d\varphi \quad (23e)$$

$$\frac{\overline{\left(\frac{\xi_t}{U}\right)^2}}{\overline{\left(\frac{u_{1,s,c}}{U}\right)^2}} = 3\tau^2 \int_0^\pi \frac{\sin\varphi\tan^2\varphi}{\Delta} d\varphi \quad (23f)$$

$$\frac{\overline{\xi^2_{x_{2,c}}} + \overline{\xi^2_{x_{3,c}}}}{\overline{\left(\frac{u_{1,s,c}}{U}\right)^2}} = 3\tau^2 \int_0^\pi \frac{\tan^4\varphi\sin\varphi}{\Delta} d\varphi \quad (23g)$$

$$\frac{\overline{\xi^2}}{\overline{\left(\frac{u_{1,s,c}}{U}\right)^2}} = 3\tau^2 \left[\frac{\int_0^\infty \Omega(k)k^2 dk}{\int_0^\infty \Omega(k)k^4 dk}\right] \int_0^\pi \frac{\sin^3\varphi}{\Delta\cos^4\varphi} d\varphi \quad (23h)$$

The subscript 1 designates a longitudinal component; subscripts 2 and 3 designate the lateral components. Of the remaining subscripts, s denotes a shear-flow component; p denotes a potential-flow component; c refers to the combustible mixture; and b refers to the burned gas. Equations (23a) to (23g) have been integrated numerically using Simpson's rule with the following increments for π: 2° intervals from 0° to 20°, 5° intervals from 20° to 70°, 2° intervals from 70° to 90°, and so forth. Numerical results are listed in table I.

TABLE I.—FLAME—TURBULENCE INTERACTION FLUCTUATION RATIOS

τ	$\sqrt{\overline{\left(\frac{u_{1,s,b}}{U}\right)^2} \Big/ \overline{\left(\frac{u_{1,s,c}}{U}\right)^2}}$ (eq. (23c))	$\sqrt{\left[\overline{\left(\frac{u_{2,s,b}}{U}\right)^2} + \overline{\left(\frac{u_{3,s,b}}{U}\right)^2}\right] \Big/ \left[\overline{\left(\frac{u_{2,s,c}}{U}\right)^2} + \overline{\left(\frac{u_{3,s,c}}{U}\right)^2}\right]}$ (eq. (23d))	$\sqrt{\overline{\left(\frac{u_{1,p,b}}{U}\right)^2} \Big/ \overline{\left(\frac{u_{1,s,c}}{U}\right)^2}}$ (eq. (23e))	$\sqrt{\overline{\left(\frac{u_{1,p,c}}{U}\right)^2} \Big/ \overline{\left(\frac{u_{1,s,c}}{U}\right)^2}}$ (eq. (23b))	$\sqrt{\overline{\left(\frac{p'_c}{\rho_c U^2}\right)^2} \Big/ \overline{\left(\frac{u_{1,s,c}}{U}\right)^2}}$ (eq. (23a))	$\sqrt{\overline{\left(\frac{\xi_t}{U}\right)^2} \Big/ \overline{\left(\frac{u_{1,s,c}}{U}\right)^2}}$ (eq. (23f))	$\left[\overline{\xi^2_{x_{2,c}}} + \overline{\xi^2_{x_{3,c}}}\right] \Big/ \overline{\left(\frac{u_{1,s,c}}{U}\right)^2}$ (eq. (23g))	$\left[-\frac{\overline{u_{3,c}}}{U}\overline{\xi_{x_{2,c}}} - \frac{\overline{u_{3,c}}}{U}\overline{\xi_{x_{3,c}}}\right] \Big/ \overline{\left(\frac{u_{1,s,c}}{U}\right)^2}$ (eq. (26))
1	1.0000	1.0000	0	0	0	1.0000	∞	1.0000
1.5	.8868	.9380	----------	----------	----------	----------	6.0062	1.9553
2	.8814	.9120	.7024	.6833	.7146	.6109	2.2942	1.4270
2.25	----------	----------	----------	----------	----------	----------	1.6501	1.2626
3	.9103	.8904	.8235	.7823	.8358	.4686	.7974	.9439
3.5	----------	----------	----------	----------	----------	----------	.5559	.8098
5	.9676	.8772	.9325	.8604	.9416	.3307	.2521	.5697
7	1.0067	.8727	.9876	.8956	.9943	.2599	.1236	.4094
10	1.0452	.8700	1.0352	.9234	1.0397	.1995	.0592	.2884
15	1.0833	.8682	1.0786	.9463	1.0813	.1462	.0260	.1930
∞	1.2247	.8660	1.2247	1.0000	1.2247	0	0	0

DISCUSSION OF RESULTS

Mean-square fluctuation quantities generated by the linearized interaction of a constant-pressure combustion front with a weak isotropic turbulence field satisfying the continuity equation for incompressible flow are given by equations (23) in terms of the incident-turbulence-velocity components. Equations (23a), (23b), and (23e) apply only at the flame front where the attenuation factors are unity. This restriction does not apply to equations (23c) and (23d) in the assumed absence of turbulent decay processes.

VELOCITY FLUCTUATIONS

Potential-flow fluctuations.—The root-mean-square velocities associated with the attenuating pressure fields generated in the combustible mixture (eq. (23b)) and in the burned gas (eq. (23e)) are plotted in figure 2. Since these

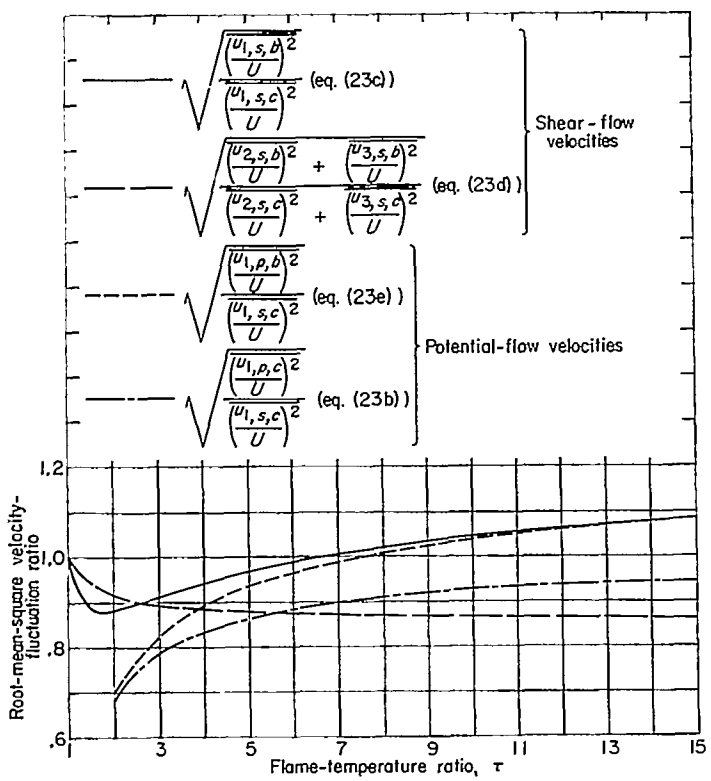

FIGURE 2.—Effect of flame-temperature ratio on shear-flow and potential-flow velocity fluctuations.

ratios apply only at the flame front where the exponential attenuation factors are unity, they represent maximum values. As is to be expected from the boundary-condition requirement of equal pressure fluctuations with differing densities on each side of the flame front, potential-flow velocity components in the burned gas exceed those in the combustible mixture. Both ratios increase with increasing flame-temperature ratio, reaching asymptotic values of $\sqrt{3/2}$ in the burned gas and 1 in the combustible mixture. Hot-wire instrumentation will respond to these fluctuation velocities as well as to the shear-flow fluctuation velocities. In view of their exponential attenuation characteristics, however, such contributions would not be of importance unless measurements were made at stations very close to the flame, that is, within a distance of the order of incident-turbulence scale. For the low flame Mach numbers encountered in combustion, the contribution to the hot-wire signal voltage of the unattenuated sound waves described in the section FLAME—TURBULENCE INTERACTION PROCESS should be quite small.

Flame-generated turbulence.—The shear flow in the burned gas (eqs. (23c) and (23d)) constitutes the flame-generated turbulence occasioned by the presence of approach-flow turbulence. These velocities, referred to the incident turbulence velocities, are also plotted in figure 2. A slight amplification of the longitudinal component occurs for values of τ over 7. In the limit, as τ becomes very large the longitudinal and lateral velocity ratios approach asymptotic values of $\sqrt{3/2}$ and $\frac{1}{2}\sqrt{3}$, respectively.

The diagrams of figure 1 indicate that a pressure wave interacting with the flame front can also bring about a shear flow in the burned gas. Although the reflection and the consequent impingement of the pressure fields described by equation (23a) upon the flame front are possible, any additions to the flame-generated turbulence level through the reflection process would probably be negligible because of the attenuating nature of the pressure field. Thus, contrary to the predictions of references 6 and 7 that the flame-generated turbulence intensity should be many times greater than the intensity of the incident field, the present analysis indicates that the two intensities are about equal.

It is interesting to note that a stream contraction (ref. 17) increases the downstream velocity of the mean flow (as does the flame front also) while exercising a different selective effect upon an incident isotropic turbulence field. For example, with a sevenfold increase in the downstream velocity of the mean flow, the longitudinal velocity ratio (in the absence of decay effects) is 1.01 for the flame front and 0.31 for the contraction. The corresponding lateral velocity ratios are 0.87 and 2.29, respectively.

TURBULENT FLAME SPEED

The higher mass-flow burning rate of a turbulent flame as compared with that of the corresponding laminar flame is generally described in terms of a turbulent flame speed U_T. The flame-speed ratio U_T/U is generally assumed to be equivalent to the ratio of turbulent-to-laminar flame surface area.

Calculation of the turbulent flame speed requires consideration of second-order terms. The local instantaneous normal propagation velocity $U+\delta U$ of the distorted flame front into the combustible mixture at rest is

$$U+\delta U=\frac{U_T+\xi_t'-u_{1,c}'+\xi_{x_2,c}'u_{2,c}'+\xi_{x_3,c}'u_{3,c}'}{\sqrt{1+\xi_{x_2,c}'^2+\xi_{x_3,c}'^2}} \tag{24}$$

Let $U_T=U+U_{\mathrm{I}}+U_{\mathrm{II}}+\ \ldots$ where U_N represents a steady-state contribution to the flame speed of order N. The perturbation quantities, for example, are written as

$$\xi_t'=\xi_t^{\mathrm{I}}+\xi_t^{\mathrm{II}}+\ \ldots$$

$$u_{1\ c}'=u_{1,c}^{\mathrm{I}}+u_{1,c}^{\mathrm{II}}+\ \ldots$$

The superscript on a fluctuation quantity ξ_t^N indicates the order of the perturbation. As before, $\delta U/U$ is taken as

$$\frac{\delta U}{U}=\frac{nr_3T_c^n}{U}\frac{T_c'}{T_c}=\frac{(\gamma-1)nr_2}{\sqrt{\gamma R_g}}(T_c)^{n-\frac{1}{2}}M\frac{p_c'}{\rho_cU^2}\equiv\Gamma\frac{p_c'}{\rho_cU^2}$$

Substitution of this expression into equation (24) and performing the indicated expansions yield the following relation, which is correct through second-order terms:

$$\underbrace{\Gamma\left(\frac{p_c^{\mathrm{I}}}{\rho_cU^2}\right)}_{\text{first-order terms}}+\underbrace{\left\{\Gamma\frac{p_c^{\mathrm{II}}}{\rho_cU^2}+\frac{1}{2}\left[(\xi^{\mathrm{I}}_{x_{2,c}})^2+(\xi^{\mathrm{II}}_{x_{3,c}})^2\right]\right\}}_{\text{second-order terms}}$$

$$=\underbrace{\left(\frac{U_{\mathrm{I}}}{U}+\frac{\xi_t^{\mathrm{I}}}{U}-\frac{u^{\mathrm{I}}_{1,c}}{U}\right)}_{\text{first-order terms}}+\underbrace{\left(\frac{U_{\mathrm{II}}}{U}+\frac{\xi_t^{\mathrm{II}}}{U}-\frac{u^{\mathrm{II}}_{1,c}}{U}+\frac{u^{\mathrm{I}}_{2,c}}{U}\xi^{\mathrm{I}}_{x_{2,c}}+\frac{u^{\mathrm{I}}_{3,c}}{U}\xi^{\mathrm{I}}_{x_{3,c}}\right)}_{\text{second-order terms}}$$

Averaging this equation yields

$$\frac{U_{\mathrm{I}}}{U}=0$$

$$\frac{U_{\mathrm{II}}}{U}=\Gamma\frac{\rho_c^{\mathrm{II}}}{\rho_cU^2}+\frac{1}{2}\left[\overline{(\xi^{\mathrm{I}}_{x_{2,c}})^2}+\overline{(\xi^{\mathrm{I}}_{x_{3,c}})^2}\right]-\overline{\frac{u^{\mathrm{I}}_{2,c}}{U}\xi^{\mathrm{I}}_{x_{2,c}}}-\overline{\frac{u^{\mathrm{I}}_{3,c}}{U}\xi^{\mathrm{I}}_{x_{3,c}}}$$

For the limiting case of constant-pressure combustion, $\Gamma=0$. Thus, the ratio of turbulent-to-laminar flame speeds can be written for this case as

$$\frac{U_T}{U}=1+\frac{1}{2}\left[(\xi^{\mathrm{I}}_{x_{2,c}})^2+(\xi^{\mathrm{I}}_{x_{3,c}})^2\right]-\left(\frac{u^{\mathrm{I}}_{2,c}}{U}\xi^{\mathrm{I}}_{x_{2,c}}+\frac{u^{\mathrm{I}}_{3,c}}{U}\xi^{\mathrm{I}}_{x_{3,c}}\right)\quad(25)$$

The first two terms on the right side of equation (25) represent the ratio of averaged turbulent-to-laminar flame surface area. The third term is a correlation coefficient representing the transverse-velocity-fluctuation contribution to the turbulent flame speed caused by flame-front distortion. It is interesting to note that only the transverse velocity fluctuations appear explicitly. The second term has already been determined (eq. (23g)). The third term may be obtained from equations (C8) as

$$-\overline{\frac{u^{\mathrm{I}}_{2,c}}{U}\xi^{\mathrm{I}}_{x_{2,c}}}-\overline{\frac{u^{\mathrm{I}}_{3,c}}{U}\xi^{\mathrm{I}}_{x_{3,c}}}=\frac{3\tau}{2}\int_0^\tau\left\{\left[\tau(\tau-1)\tan^4\varphi+(\tau^2+1)\tan^2\varphi+(\tau+1)\right]\frac{\sin^3\varphi}{\Delta}+iQ\right\}d\varphi\quad(26)$$

The imaginary term has not been written out inasmuch as it does not contribute to the integral. The results of the indicated integrations are listed in table I.

Equation (25) for the flame-speed ratio U_T/U may also be written in the form

$$\frac{U_T}{U}=1+S\frac{\overline{u^2_{1,3,c}}}{U^2}\quad(27)$$

where the flame-speed parameter S is obtained from the values listed in table I from equations (23g) and (26). The variation of this parameter with the flame-temperature ratio τ shown in figure 3 suggests, on the assumption that the flame-front slopes $\xi_{x_{2,c}}$ and $\xi_{x_{3,c}}$ govern contributions to the right side of equation (25), that the flame front with the higher heat release is distorted less by a given intensity of turbulence. For the degenerate case $\tau=1$ (no heat release), the parameter S becomes infinite—a condition compatible with this viewpoint.

The present analysis requires that the flame-front slopes, as well as the other perturbation quantities, be small. The preceding discussion suggests that the incremental flame-speed ratio $(U_T-U)/U$ may be of the second order as a result of this restriction to small flame-front slopes.

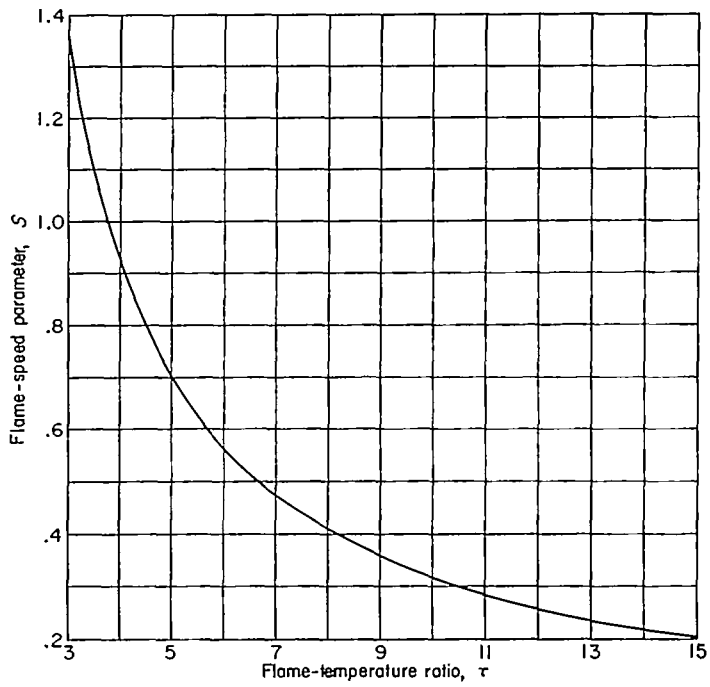

FIGURE 3.—Effect of flame-temperature ratio on flame speed for incident isotropic turbulence.

COMBUSTION NOISE

The root-mean-square pressure-fluctuation coefficient $\sqrt{\overline{p_c'^2}}/\rho_cU^2$, which applies directly at the flame front, is plotted in figure 4 for the limiting case of constant-pressure combustion. The pressure fluctuations are a measure of the random noise generated by the interaction of the flame front with the incident turbulence. In acoustical measurements, the noise level in decibels is usually given with respect to a reference pressure of 0.0002 dyne per square centimeter (ref. 18), which corresponds approximately to the pressure amplitude of a plane sound wave of minimum audible intensity at a frequency of 1000 cycles per second. The noise-pressure level in decibels is defined by the relation

$$\text{Noise-pressure level}\equiv 20\log_{10}\left(\frac{\sqrt{\overline{p_c'^2}}}{0.0002}\right)=74+20\log_{10}\sqrt{\overline{p_c'^2}}\quad(28)$$

where the pressure fluctuations in the combustible mixture are given in dynes per square centimeter.

TABLE II.—HYDROCARBON-AIR FLAME DATA AT SPECIFIED CONDITIONS

[Static pressure and temperature of combustible mixture, 760 mm Hg and 25° C, respectively.]

	Propane, C_3H_8		Ethylene, C_2H_4		Acetylene, C_2H_2	
	At stoichiometric	At maximum U	At stoichiometric	At maximum U	At stoichiometric	At maximum U
Fuel-air ratio	0.0638	0.0721	0.0676	0.0757	0.0753	0.1040
Fuel in air, percent by volume	4.04	4.54	6.54	7.65	7.75	10.70
Laminar flame speed, U, cm/sec	37.5	39	64	68	123.5	141
Adiabatic flame-temperature ratio, τ	7.70	7.45	7.95	8.00	8.64	8.71

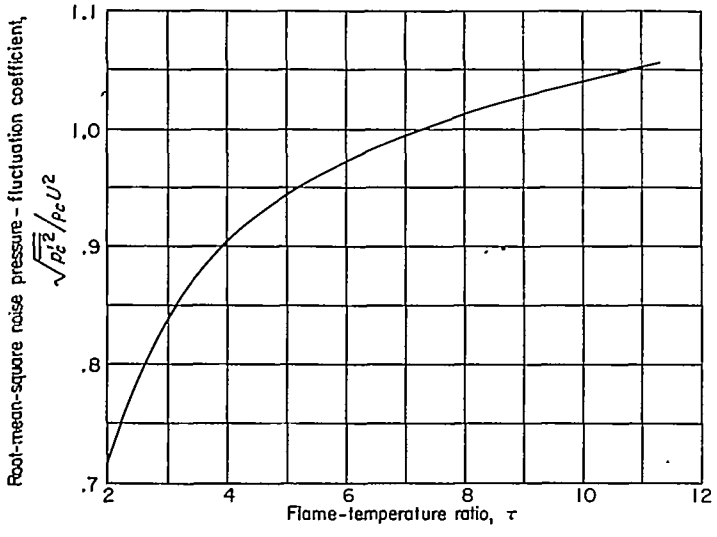

FIGURE 4.—Effect of flame-temperature ratio on random pressure fluctuations generated at flame front.

Equations (23a) and (28) indicate that the noise level should be particularly dependent upon flame speed. Propane-air and acetylene-air combustions, which are characterized by a low flame speed and a fairly high flame speed, respectively, will be considered for illustrative purposes. Pertinent data for these flames at maximum-flame-speed and stoichiometric conditions for an ambient temperature of 25° C and a pressure of 760 millimeters of mercury are given in table II. The adiabatic equilibrium flame temperatures, at which the total enthalpy of the fuel and oxidant equals the total enthalpy of the products of reaction, were calculated using the procedure of reference 19. (Total enthalpy includes the chemical contributions to the internal energy.) Flame-speed data were obtained from references 20 and 21.

If the flame-front turbulence intensity $\sqrt{\overline{u_{1,s,c}^2}}/U$ is assumed equal to 10 percent, noise-pressure levels of 59 and 81 decibels are obtained for propane-air flames and acetylene-air flames, respectively, under conditions for maximum laminar flame speed. At an approach-flow velocity of 1225 centimeters per second, which is in the range of velocities usually encountered in combustion experiments, the corresponding intensity of the approach-flow turbulence would be about 0.3 percent for the propane-air mixture and about 1 percent for the acetylene-air mixture.

Thus, the pressure fluctuations generated at the flame front when the incident turbulence is of low intensity, although small compared with ambient pressure, are apparently of fairly high acoustical intensity for constant-pressure combustion. Because of the exponential attenuation of these pressure fields, the "far-field" acoustic intensity (the intensity at distances very far from the flame front) approaches zero. For cases other than constant-pressure combustion, a finite "far-field" intensity is obtained.

CONCLUDING REMARKS

The present linearized analysis has treated the interaction of a field of isotropic turbulence with a free flame front under constant-pressure combustion conditions with no turbulence decay processes or heat-release fluctuations. The interaction produces an anisotropic turbulence field in the burned gas which has axisymmetry about the mainstream direction. Contrary to the results predicted by several current theories of turbulent flame speed, the flame-generated turbulence velocities caused by approach-flow turbulence do not differ greatly from the turbulence velocities of the incident field.

The incremental flame-speed ratio $(U_T - U)/U$ as obtained from the present analysis is a second-order quantity consisting of two parts. One part represents the root-mean-square area of the turbulent flame front; the other represents the contribution of the transverse velocity fluctuations which result from the flame-front distortion. The flame-speed ratio U_T/U for a given level of incident turbulence intensity $\sqrt{\overline{u_{1,s,c}^2}}/U$ is found to decrease with increasing heat-release rates (increasing values of τ).

Random pressure fluctuations generated in both the combustible mixture and the burned gas, although small compared with ambient pressure, give rise to appreciable noise levels (59 to 81 db) directly at the flame front even for very moderate intensities of approach-flow turbulence (flame-front turbulence intensities of 10 percent). For the limiting case of constant-pressure combustion, the pressure waves attenuate exponentially with distance from the flame front, so that the "far-field" intensity approaches zero.

LEWIS FLIGHT PROPULSION LABORATORY
NATIONAL ADVISORY COMMITTEE FOR AERONAUTICS
CLEVELAND, OHIO, *January 25, 1955*

APPENDIX A

SYMBOLS

A	magnitude of two-dimensional vorticity-wave velocity vector in combustible mixture
$\underline{A}$	two-dimensional vorticity-wave velocity vector in combustible mixture
a	speed of sound
B_1,B_2,B_3	coefficients defined in eqs. (4)
b	constant defined in eqs. (7) and (9)
C	amplitude of combustible mixture shear-wave component parallel to $x_{3,c}$-axis
c	constant defined in eqs. (7) and (9)
c_p	specific heat at constant pressure
c_v	specific heat at constant volume
D_1	$U/(U-V)$, eqs. (4)
d	constant defined in eqs. (7) and (9)
E_1	$-V/U$, eqs. (4)
$F_{ij}(\underline{k},t)$	spectral tensor function
f	constant defined in eqs. (7) and (9)
G	$(G_1+iG_2)/A \sin \varphi$
G_1,G_2	amplitude coefficients of shear-wave longitudinal component in burned gas
H	$(H_1+iH_2)/A \sin \varphi$
H_1,H_2	amplitude coefficients of flame-front displacement
$h_1,h_2 \ldots h_{10}$	groupings defined in eqs. (B16)
I_1,I_2	amplitude coefficients of shear-wave transverse component in burned gas
J_1,J_2	amplitude coefficients of pressure wave in burned gas
$J^{(1)},J^{(2)}$	$J^{(1)} \equiv \frac{p_b}{\rho_c U^2} J_1$; $J^{(2)} \equiv \frac{p_b}{\rho_c U^2} J_2$, eq. (10d)
K_1,K_2,K_3,K_4	coefficients defined in eqs. (4)
k	magnitude of wave-number vector $\underline{k}$
k	wave-number vector of shear wave in combustible mixture with components k_1',k_2' in x_c,y-coordinate system, with components k_1, k_2, k_3 in $x_{1,c}$, $x_{2,c}$, $x_{3,c}$-coordinate system
L_1,L_2	amplitude coefficients of density associated with shear entropy wave in burned gas
M	flame-front Mach number, $M \equiv U/a_c$
m^2	$a_2/\gamma U^2$, eq. (B16)
N	$(N_1+iN_2)/A \sin \varphi$
N_1,N_2	amplitude coefficients of longitudinal velocity component associated with pressure wave in burned gas
n	exponent used in representation of laminar flame speed as function of combustible-mixture static temperature
P_1,P_2	amplitude coefficients of lateral velocity component associated with pressure wave in burned gas
p	static pressure
p'	static-pressure perturbation
Q	term not contributing to the integral in eq. (26)
R	$(R^{(1)}+R^{(2)})/A \sin \varphi$
R_g	gas constant
R_1,R_2	amplitude coefficients of pressure wave in combustible mixture
$R^{(1)},R^{(2)}$	$R^{(1)} \equiv R_1/\gamma M^2, R^{(2)} = R_2/\gamma M^2$, eq. (10c)
$\underline{r}$	separation vector
r_1,r_2	constants used in representation of laminar flame speed as function of combustible-mixture static temperature
S	flame-speed parameter, eq. (27)
T	static temperature
$T_{ij}(\underline{r},t)$	velocity correlation tensor for homogeneous turbulence
T_S	stagnation temperature
t	time
U	laminar or fundamental flame speed
U_T	mean turbulent flame speed
u'	longitudinal component of velocity perturbation
$u_{1,c}, u_{2,c}, u_{3,c}$	velocity perturbation components in combustible mixture parallel to $x_{1,c},x_{2,c},x_{3,c}$-coordinate axes, respectively
$u_{1,b}, u_{2,b}, u_{3,b}$	velocity perturbation components in burned gas parallel to $x_{1,b},x_{2,b},x_{3,b}$-coordinate axes, respectively
V	mean velocity of burned gas
V_T	mean velocity of burned gas in turbulent combustion
v'	lateral component of velocity perturbation
W	$(W_1+iW_2)/A \sin \varphi$
W_1, W_2	amplitude coefficients of longitudinal velocity component associated with pressure wave in combustible mixture
w'	lateral component of velocity perturbation (component parallel to plane of unperturbed flame front and normal to u' and v' components)
X_1, X_2	amplitude coefficients of lateral velocity component associated with pressure wave in combustible mixture
$\underline{x}$	position vector
x_b	coordinate in x_b,y-system measured in direction of unperturbed flame-front travel relative to which burned gas is at rest
x_c	coordinate in x_c,y-system measured in direction of unperturbed flame-front travel relative to which combustible mixture is at rest
$x_{1,b}$	coordinate in $x_{1,b},x_{2,b},x_{3,b}$-system measured in direction of unperturbed flame-front travel relative to which burned gas is at rest
$x_{2,b}$	coordinate orthogonal to $x_{1,b}$ and $x_{3,b}$ and making angle θ with y-coordinate
$x_{3,b}$	coordinate orthogonal to $x_{1,b}$ and $x_{2,b}$

$x_{1,c}$ coordinate in $x_{1,c},x_{2,c},x_{3,c}$-system measured in direction of unperturbed flame-front travel relative to which combustible mixture is at rest

$x_{2,c}$ coordinate orthogonal to $x_{1,c}$ and $x_{3,c}$ and making angle θ with y-coordinate

$x_{3,c}$ coordinate orthogonal to $x_{1,c}$ and $x_{2,c}$

y coordinate orthogonal to x_c and x_b

$d\underline{Z}_i(\underline{k},t)$ random amplitude vector of shear-field Fourier component

z coordinate orthogonal to x_c and y

$\alpha_1,\alpha_2 \ldots \alpha_5$ grouping defined in eqs. (B18)

Γ $\dfrac{(\gamma-1)nr_2(T_c)^{n-\frac{1}{2}}M}{\sqrt{\gamma R_g}}$

γ ratio of specific heats

Δ $\tau^2(\tau-1)^2\tan^4\varphi+2\tau(\tau^2+2\tau-1)\tan^2\varphi+(\tau+1)^2$

$\delta_1,\delta_2 \ldots \delta_6$ grouping defined in eqs. (B24)

$\epsilon_1,\epsilon_2 \ldots \epsilon_{10}$ grouping defined in eqs. (B21)

ζ variable upon which pressure wave depends, eqs. (7)

η variable upon which pressure wave depends, eqs. (7)

θ angle between polarization plane of incident shear wave and $x_{1,c},x_{2,c}$-plane

Λ coefficient defined in eq. (3e)

ν $k_1'x_c+k_2'y$

$\xi'(y,t)$ flame-front displacement

$'$ flame-front displacement velocity

$\xi'_{x_{2,c}}$ flame-front slope with respect to $x_{2,c}$-coordinate

$\xi'_{x_{3,c}}$ flame-front slope with respect to $x_{3,c}$-coordinate

ξ'_y flame-front slope with respect to y-coordinate

ρ static density

ρ' static-density perturbation

σ $k_1'Ut+k_2'y$, eq. (10j)

τ flame-temperature ratio, $T_{s,b}/T_{s,c}$

$\Phi_{ij}(\underline{k},t)$ spectral density tensor

φ angle between wave-number vector of incident shear wave and direction of unperturbed flame-front travel, $\tan\varphi\equiv k_2'/k_1'$

ψ $\left(\dfrac{U}{U-V}\right)k_1'x_b+k_2'y$

Ω scalar amplitude function defining spectral density tensor

Subscripts:

b burned gas

c combustible mixture

cr critical

p potential-flow velocity component

s shear-flow velocity component

1,2,3 orthogonal coordinate designation

I,II designates order of steady-flow quantity

Superscripts:

I,II designates order of fluctuation quantity

$*$ denotes complex conjugate

$'$ denotes fluctuation quantity except where otherwise specified

APPENDIX B

ATTENUATING-WAVE SOLUTION FOR SINGLE-WAVE INTERACTION

The arguments of the various fluctuation quantities are equal at the flame front where $x_c=Ut$ and $x_b=(U-V)t$. Therefore, substituting equations (10) into equations (3) and (5) and separately equating the real terms and the imaginary terms provide the following set of equations:

$$\left.\begin{aligned} J_1\left(1+\frac{B_1}{\gamma}\right)+B_1L_1-B_2N_1-B_2G_1&=\\ -B_2A\sin\varphi-B_2W_1+B_3R_1&\\ J_2\left(1+\frac{B_1}{\gamma}\right)+B_1L_2-B_2N_2-B_2G_2=-B_2W_2+B_3R_2& \end{aligned}\right\} \quad \text{(B1)}$$

$$\left.\begin{aligned} J_1\left(1-\frac{1}{\gamma}\right)-L_1-K_1N_1-K_1G_1=-K_4W_1-&\\ K_4A\sin\varphi+K_2R_1+K_3\tau'-(K_1-K_4)H_1&\\ J_2\left(1-\frac{1}{\gamma}\right)-L_2-K_1N_2-K_1G_2=&\\ -K_4W_2+K_2R_2-(K_1-K_4)H_2& \end{aligned}\right\} \quad \text{(B2)}$$

$$\left.\begin{aligned} \frac{1}{\gamma}J_1+L_1+(D_1-1)H_1-D_1N_1-D_1G_1=&\\ -W_1-A\sin\varphi+\frac{1}{\gamma}R_1&\\ \frac{1}{\gamma}J_2+L_2+(D_1-1)H_2-D_1N_2-D_1G_2=-W_2+\frac{1}{\gamma}R_2& \end{aligned}\right\} \quad \text{(B3)}$$

$$\left.\begin{aligned} P_1+I_1=X_1-\frac{k_1'}{k_2'}A\sin\varphi+\frac{k_2'}{k_1'}E_1H_1&\\ P_2+I_2=X_2+\frac{k_2'}{k_1'}E_1H_2& \end{aligned}\right\} \quad \text{(B4)}$$

$$\left.\begin{aligned} -f_b\left(\frac{U-V}{U}\right)N_1-d_bN_2=m^2(-f_bJ_1+b_bJ_2)&\\ d_bN_1-f_b\left(\frac{U-V}{U}\right)N_2=m^2(-b_bJ_1-f_bJ_2&\end{aligned}\right\} \quad \text{(B5)}$$

$$\left.\begin{aligned} -f_b\left(\frac{U-V}{U}\right)P_1-d_bP_2=m^2c_bJ_2&\\ d_bP_1-f_b\left(\frac{U-V}{U}\right)P_2=-m^2c_bJ_1&\end{aligned}\right\} \quad \text{(B6)}$$

$$\left.\begin{aligned} -k_1\left(\frac{U}{U-V}\right)G_2=k_2I_2&\\ -k_1\left(\frac{U}{U-V}\right)G_1=k_2I_1&\end{aligned}\right\} \quad \text{(B7)}$$

$$\left.\begin{aligned} f_cW_1-d_cW_2&=\frac{1}{\gamma M^2}(f_cR_1+b_cR_2)\\ d_cW_1+f_cW_2&=\frac{1}{\gamma M^2}(-b_cR_1+f_cR_2)\end{aligned}\right\} \quad (B8)$$

$$\left.\begin{aligned} f_cX_1-d_cX_2&=\frac{1}{\gamma M^2}c_cR_2\\ d_cX_1+f_cX_2&=-\frac{1}{\gamma M^2}c_cR_1\end{aligned}\right\} \quad (B9)$$

$$\left.\begin{aligned} H_1-W_1-A\sin\varphi&=\Lambda R_1\\ H_2-W_2&=\Lambda R_2\end{aligned}\right\} \quad (B10)$$

From equations (B5), (B6), (B8), (B9), and (B10),

$$\left.\begin{aligned} N_1&=h_1(h_2J_1-h_3J_2)\\ N_2&=h_1(h_3J_1+h_2J_2)\end{aligned}\right\} \quad (B11)$$

$$\left.\begin{aligned} P_1&=h_1(-h_4J_1-h_5J_2)\\ P_2&=h_1(h_5J_1-h_4J_2)\end{aligned}\right\} \quad (B12)$$

$$\left.\begin{aligned} W_1&=h_6(h_7R_1+h_8R_2)\\ W_2&=h_6(-h_8R_1+h_7R_2)\end{aligned}\right\} \quad (B13)$$

$$\left.\begin{aligned} X_1&=h_6(-h_9R_1+h_{10}R_2\\ X_2&=h_6(-h_{10}R_1-h_9R_2\end{aligned}\right\} \quad (B14)$$

$$\left.\begin{aligned} H_1&=\Lambda R_1+A\sin\varphi+h_6(h_7R_1+h_8R_2)\\ H_2&=\Lambda R_2+h_6(-h_8R_1+h_7R_2)\end{aligned}\right\} \quad (B15)$$

where

$$\left.\begin{aligned} h_1&\equiv\frac{m^2}{f_b^2/D_1^2+d_b^2} & h_6&\equiv\frac{1}{\gamma M^2(f_c^2+d_c^2)}\\ h_2&\equiv\frac{f_b^2}{D_1}-b_bD_b & h_7&\equiv f_c^2-b_cd_c\\ h_3&\equiv\frac{b_bf_b}{D_1}+d_bf_b & h_8&\equiv b_cf_c+d_cf_c\\ h_4&\equiv c_bd_b & h_9&\equiv c_cd_c\\ h_5&\equiv\frac{c_bf_b}{D_1} & h_{10}&\equiv c_cf_c\\ & & m^2&\equiv a_b^2/\gamma U^2\end{aligned}\right\} \quad (B16)$$

From equations (B4), (B7), (B12), (B14), and (B15),

$$\left.\begin{aligned} G_1&=\alpha_1R_1-\alpha_2R_2-\alpha_3J_1-\alpha_4J_2+\alpha_5A\sin\varphi\\ G_2&=\alpha_2R_1+\alpha_1R_2+\alpha_4J_1-\alpha_3J_2\end{aligned}\right\} \quad (B17)$$

where

$$\left.\begin{aligned} \alpha_1&\equiv\frac{k_2'}{k_1'D_1}\left[\frac{-k_2'E_1}{k_1'}(\Lambda+h_6h_7)+h_6h_9\right]\\ \alpha_2&\equiv\frac{k_2'}{k_1'D_1}\left[\frac{k_2'E_1}{k_1'}h_6h_8+h_6h_{10}\right]\\ \alpha_3&\equiv\frac{k_2'}{k_1'D_1}h_1h_4\\ \alpha_4&\equiv\frac{k_2'}{k_1'D_1}h_1h_5\\ \alpha_5&\equiv\frac{1}{D_1}\left[1-\frac{(k_2')^2}{(k_1')^2}E_1\right]\end{aligned}\right\} \quad (B18)$$

Then, from equation (B2),

$$\left.\begin{aligned} L_1=&J_1\left[1-\frac{1}{\gamma}-K_1(h_1h_2-\alpha_3)\right]+J_2[K_1(h_1h_3+\alpha_4)]+\\ &R_1[K_1(h_6h_7-\alpha_1)-K_2+(K_1-K_4)\Lambda]+\\ &R_2[K_1(h_6h_8+\alpha_2)]+A\sin\varphi[K_1(1-\alpha_5)]-K_3\tau'\\ L_2=&-J_1[K_1(h_1h_3+\alpha_4)]+J_2\left[1-\frac{1}{\gamma}-K_1(h_1h_2-\alpha_3)\right]-\\ &R_1[K_1(h_6h_8+\alpha_2)]+R_2[K_1(h_6h_7-\alpha_1)-K_2+\\ &(K_1-K_4)\Lambda]\end{aligned}\right\} \quad (B19)$$

The various disturbance amplitude coefficients of equations (10) have now been obtained in terms of the coefficients R_1, R_2, J_1, J_2 and the parameters $A\sin\varphi$ and τ'. From equations (B1) and (B3),

$$\left.\begin{aligned} J_1\epsilon_1+J_2\epsilon_2+R_1\epsilon_3+R_2\epsilon_4&=\epsilon_5\\ -J_1\epsilon_2+J_2\epsilon_1-R_1\epsilon_4+R_2\epsilon_3&=0\\ J_1\epsilon_6+J_2\epsilon_7+R_1\epsilon_8+R_2\epsilon_9&=\epsilon_{10}\\ -J_1\epsilon_7+J_2\epsilon_6-R_1\epsilon_9+R_2\epsilon_8&=0\end{aligned}\right\} \quad (B20)$$

where

$$\left.\begin{aligned} \epsilon_1&\equiv1+B_1-(B_1K_1+B_2)(h_1h_2-\alpha_3)\\ \epsilon_2&\equiv(B_1K_1+B_2)(h_1h_3+\alpha_4)\\ \epsilon_3&\equiv(B_1K_1+B_2)(h_6h_7-\alpha_1)+B_1(K_1-K_4)\Lambda-B_3-B_1K_2\\ \epsilon_4&\equiv(B_1K_1+B_2)(h_6h_8+\alpha_2)\\ \epsilon_5&\equiv B_1K_3\tau'-A\sin\varphi[(B_1K_1+B_2)(1-\alpha_5)]\\ \epsilon_6&\equiv1-(D_1+K_1)(h_1h_2-\alpha_3)\\ \epsilon_7&\equiv(D_1+K_1)(h_1h_3+\alpha_4)\\ \epsilon_8&\equiv(D_1+K_1)(h_6h_7-\alpha_1)+(D_1-1)\Lambda-K_2+\frac{1}{\gamma}+(K_1-K_4)\Lambda\\ \epsilon_9&\equiv(D_1+K_1)(h_6h_8+\alpha_2)\\ \epsilon_{10}&\equiv K_3\tau'-A\sin\varphi(D_1+K_1)(1-\alpha_5)\end{aligned}\right\} \quad (B21)$$

$$J_1=\frac{R_1(\epsilon_1\epsilon_9-\epsilon_4\epsilon_6)-R_2(\epsilon_1\epsilon_8-\epsilon_3\epsilon_6)}{\epsilon_2\epsilon_6-\epsilon_1\epsilon_7}$$
$$J_2=\frac{R_1(\epsilon_2\epsilon_9-\epsilon_4\epsilon_7)-R_3(\epsilon_2\epsilon_8-\epsilon_3\epsilon_7)}{\epsilon_2\epsilon_6-\epsilon_1\epsilon_7} \qquad \text{(B22)}$$

$$R_1=\frac{\delta_2\delta_6-\delta_3\delta_5}{\delta_2\delta_4-\delta_1\delta_5}$$
$$R_2=\frac{\delta_1\delta_6-\delta_3\delta_4}{\delta_2\delta_4-\delta_1\delta_5} \qquad \text{(B23)}$$

where

$$\delta_1\equiv\epsilon_1(\epsilon_1\epsilon_9-\epsilon_4\epsilon_6)+\epsilon_3(\epsilon_2\epsilon_6-\epsilon_1\epsilon_7)-\epsilon_2(\epsilon_4\epsilon_7-\epsilon_2\epsilon_9)$$
$$\delta_2\equiv\epsilon_1(\epsilon_1\epsilon_8-\epsilon_3\epsilon_6)-\epsilon_4(\epsilon_2\epsilon_6-\epsilon_1\epsilon_7)-\epsilon_2(\epsilon_3\epsilon_7-\epsilon_2\epsilon_8)$$
$$\delta_3\equiv\epsilon_5(\epsilon_2\epsilon_6-\epsilon_1\epsilon_7)$$
$$\delta_4\equiv\epsilon_6(\epsilon_1\epsilon_9-\epsilon_4\epsilon_6)+\epsilon_8(\epsilon_2\epsilon_6-\epsilon_1\epsilon_7)-\epsilon_7(\epsilon_4\epsilon_7-\epsilon_2\epsilon_9)$$
$$\delta_5\equiv\epsilon_6(\epsilon_1\epsilon_8-\epsilon_3\epsilon_6)-\epsilon_7(\epsilon_3\epsilon_7-\epsilon_2\epsilon_8)-\epsilon_9(\epsilon_2\epsilon_6-\epsilon_1\epsilon_7)$$
$$\delta_6\equiv\epsilon_{10}(\epsilon_2\epsilon_6-\epsilon_1\epsilon_7) \qquad \text{(B24)}$$

Equations (B11) to (B15), (B17), (B19), (B22), and (B23) provide the formal solution of equations (B1) to (B10).

APPENDIX C

ATTENUATING-WAVE SOLUTION FOR CONSTANT-PRESSURE COMBUSTION

If terms of order M^2 are retained, equations (1) provide the following relations for the unperturbed-flow quantities:

$$\frac{p_b}{p_c}=1-\gamma(\tau-1)M^2+\ldots$$
$$\frac{\rho_c}{\rho_b}=\frac{U-V}{U}=\tau\left[1+\frac{\gamma+1}{2}(\tau-1)M^2+\ldots\right]$$
$$\frac{c_pT_{S,c}}{U^2}=\frac{1}{2}+\frac{1}{(\gamma-1)M^2}$$
$$\frac{U^2}{a_b^2}=\frac{2M^2}{\tau[2-(\gamma-1)(\tau-1)M^2-(\gamma^2-1)\tau(\tau-1)M^4+\ldots]}$$

With these relations, equations (4) take the form

$$B_1=\gamma\tau M^2,\ B_2=2\gamma M^2,\ B_3=1+[1+\gamma(\tau-1)]M^2$$
$$D_1=\frac{1}{\tau}\left[1-\frac{\gamma+1}{2}(\tau-1)M^2\right],\ E_1=(\tau-1)\left[1+\frac{\gamma+1}{2}\tau M^2\right]$$
$$K_1=K_4=(\gamma-1)M^2,\ K_2=\frac{\gamma-1}{\gamma}\left[1+\frac{\gamma-1}{2}(\tau-1)M^2\right],\ K_3=\frac{1}{\tau}+\frac{\gamma-1}{2}M^2 \qquad \text{(C1)}$$

and equations (9) may be written

$$b_c=b_b=-k_1'M^2,\ c_c=c_b=k_2',\ d_c=k_1'(1+M^2),\ d_b=k_1'(1+\tau M^2)$$
$$f_c^2=(k_2')^2-[(k_1')^2-(k_2')^2]M^2,\ f_b^2=(k_2')^2-\left[\frac{(k_1')^2-\tau^2(k_2')^2}{\tau}\right]M^2 \qquad \text{(C2)}$$

If only the leading terms in powers of M^2 are retained, equations (B16) and (B18) provide the following relations:

$$h_1h_2=h_1h_5=\frac{\tau^2\tan^2\varphi}{\gamma M^2(1+\tau^2\tan^2\varphi)},\quad h_1h_3=h_1h_4=\frac{\tau\tan\varphi}{\gamma M^2(1+\tau^2\tan^2\varphi)}$$
$$h_6h_7=h_6h_{10}=\frac{\sin^2\varphi}{\gamma M^2},\qquad h_6h_8=h_6h_9=\frac{\sin\varphi\cos\varphi}{\gamma M^2} \qquad \text{(C3)}$$

and

$$\alpha_1=\frac{\tau\sin^2\varphi}{\gamma M^2}[1-(\tau-1)\tan^2\varphi]$$
$$\alpha_2=\frac{\tau^2\sin^2\varphi\tan\varphi}{\gamma M^2}$$
$$\alpha_3=\frac{\tau^2\tan^2\varphi}{\gamma M^2(1+\tau^2\tan^2\varphi)}$$
$$\alpha_4=\frac{\tau^3\tan^3\varphi}{\gamma M^2(1+\tau^2\tan^2\varphi)}$$
$$\alpha_5=\tau[1-(\tau-1)\tan^2\varphi] \qquad \text{(C4)}$$

From these relations:

$$h_1h_3+\alpha_4=\frac{\tau\tan\varphi}{\gamma M^2},\quad h_6h_7-\alpha_1=\frac{(\tau-1)\sin^2\varphi(\tau\tan^2\varphi-1)}{\gamma M^2}$$
$$h_1h_2-\alpha_3=0,\qquad h_6h_8+\alpha_2=\frac{\sin\varphi\cos\varphi(1+\tau^2\tan^2\varphi)}{\gamma M^2} \qquad \text{(C5)}$$

From equations (B21) and (C5),

$$\epsilon_1\epsilon_9-\epsilon_4\epsilon_6=\frac{\sin\varphi\cos\varphi(1+\tau^2\tan^2\varphi)}{\gamma M^2\tau}$$
$$\epsilon_1\epsilon_8-\epsilon_3\epsilon_6=\frac{(\tau-1)\sin^2\varphi(\tau\tan^2\varphi-1)}{\gamma M^2\tau}$$
$$\epsilon_3\epsilon_7-\epsilon_2\epsilon_8=\epsilon_2\epsilon_6-\epsilon_1\epsilon_7=-\frac{\tan\varphi}{\gamma M^2},\ \epsilon_4\epsilon_7-\epsilon_2\epsilon_9=0 \qquad \text{(C6)}$$

and from equations (B21), (B24), and (C6):

$$\left.\begin{aligned}
\delta_1&=\frac{\sin\varphi\cos\varphi}{\gamma M^2\tau}[(\tau+1)(1+\tau\tan^2\varphi)-\\
&\qquad 2\tan^2\varphi(\tau-1)\tau(\tau\tan^2\varphi-1)]\\
\delta_2&=\frac{\sin^2\varphi}{\gamma M^2\tau}[(\tau-1)(\tau\tan^2\varphi-1)+2(\tau+1)\tau(\tau\tan^2\varphi+1)]\\
\delta_3&=-\tan\varphi[\tau'-2(\tau-1)(\tau\tan^2\varphi-1)A\sin\varphi]\\
\delta_4&=\frac{-(\tau-1)\tan\varphi\sin^2\varphi(\tau\tan^2\varphi-1)}{\gamma^2M^4\tau}\\
\delta_5&=\frac{(\tau+1)(\tau\tan^2\varphi+1)\sin^2\varphi}{\gamma^2M^4\tau}\\
\delta_6&=-\frac{\tan\varphi}{\gamma M^2\tau}[\tau'-(\tau-1)(\tau\tan^2\varphi-1)A\sin\varphi]
\end{aligned}\right\}\quad(C7)$$

Since for constant-pressure combustion $R^{(1)}\equiv R_2/\gamma M^2$, $R^{(2)}\equiv R_2/\gamma M^2$, and so forth, the coefficients $R^{(1)}$, $R^{(2)}$, $J^{(1)}$, and $J^{(2)}$ are obtained from equations (B22), (B23), (C6), and (C7). With these coefficients determined, the remainder are obtained from equations (B7), (B11) to (B14), (B17), and (B19). The amplitude coefficients are

$$\left.\begin{aligned}
R^{(1)}&=\frac{-1}{\Delta}\left\{(\tau-1)^2(\tau\tan^2\varphi-1)^2A\sin\varphi-[\tau^2(\tau^2+2\tau-1)\tan^2\varphi+\tau(\tau^2+1)]\frac{\tau'}{\tau}\right\}\\
R^{(2)}&=J^{(2)}=-\frac{1}{\Delta\tan\varphi}\left\{(\tau^2-1)(\tau^2\tan^4\varphi-1)A\sin\varphi+[\tau^3(\tau-1)\tan^4\varphi-2\tau^3\tan^2\varphi-\tau(\tau+1)]\frac{\tau'}{\tau}\right\}\\
J^{(1)}&=-\frac{1}{\Delta}\left\{(\tau-1)^2(\tau\tan^2\varphi-1)^2A\sin\varphi+\tau^2[\tau(\tau-1)^2\tan^4\varphi+(\tau^2+2\tau-1)\tan^2\varphi+2]\frac{\tau'}{\tau}\right\}\\
L_1&=-\frac{\tau'}{\tau},\ L_2=0\\
N_1&=\frac{\tau}{\Delta(1+\tau^2\tan^2\varphi)}\Big((\tau-1)(\tau\tan^2\varphi-1)[(\tau+1)(\tau\tan^2\varphi+1)-\tau(\tau-1)\tan^2\varphi(\tau\tan^2\varphi-1)]A\sin\varphi-\\
&\qquad\tau\left\{\tau^2\tan^2\varphi[\tau(\tau-1)^2\tan^4\varphi+\tau(\tau+1)\tan^2\varphi+4]+(\tau+1)\right\}\frac{\tau'}{\tau}\Big)\\
N_2&=\frac{-\tau(\tau-1)\tan\varphi}{\Delta(1+\tau^2\tan^2\varphi)}\left\{(\tau\tan^2\varphi-1)[\tau(\tau+1)(\tau\tan^2\varphi+1)+(\tau-1)(\tau\tan^2\varphi-1)]A\sin\varphi+\right.\\
&\qquad\left.\tau^2[\tau(2\tau-1)\tan^4\varphi-(\tau-1)\tan^2\varphi-1]\frac{\tau'}{\tau}\right\}\\
G_1&=\frac{\tau}{\Delta(1+\tau^2\tan^2\varphi)}\left\{[(\tau+1)^2(\tau\tan^2\varphi+1)^2+\tau(\tau-1)^2\tan^2\varphi(\tau\tan^2\varphi-1)^2]A\sin\varphi-\right.\\
&\qquad\left.\tau(\tau-1)\tan^2\varphi[\tau(\tau^2+2\tau-1)\tan^2\varphi+(\tau^2+1)]\frac{\tau'}{\tau}\right\}\\
G_2&=\frac{(\tau-1)\tan\varphi}{\Delta(1+\tau^2\tan^2\varphi)}\left\{(\tau^2-1)(\tau\tan^2\varphi-1)(\tau\tan^2\varphi+1)A\sin\varphi+[\tau^3(\tau-1)\tan^4\varphi-2\tau^3\tan^2\varphi-\tau(\tau+1)]\frac{\tau'}{\tau}\right\}\\
P_1&=-N_2,\ P_2=N_1\\
I_1&=\frac{G_1}{\tau\tan\varphi},\ I_2=\frac{-G_2}{\tau\tan\varphi}\\
W_1&=-\frac{1}{\Delta}\left\{(\tau-1)(\tau\tan^2\varphi-1)[\tau(\tau-1)\tan^2\varphi+(\tau+1)]A\sin\varphi-[\tau^2(3\tau-1)\tan^2\varphi+\tau(\tau+1)]\frac{\tau'}{\tau}\right\}\\
W_2&=-\frac{\tau(\tau-1)\tan\varphi}{\Delta}\left\{2(\tau\tan^2\varphi-1)A\sin\varphi+\tau[\tau\tan^2\varphi+1]\frac{\tau'}{\tau}\right\}\\
X_1&=H_2=W_2,\ X_2=-W_1\\
H_1&=\frac{\tau}{\Delta}\left\{2(\tau+1)(\tau\tan^2\varphi+1)A\sin\varphi+[\tau(3\tau-1)\tan^2\varphi+(\tau+1)]\frac{\tau'}{\tau}\right\}
\end{aligned}\right\}\quad(C8)$$

For constant-pressure combustion, $\zeta_c=\zeta_b=k_1'Ut+k_2'y$, $\eta_c=k_2'(x_c-Ut)$, $\eta_b=k_2'[-x_b+(U-V)t]$, $\nu=k_1'x_c+k_2'y$, $\psi=\frac{k_1'x_b}{\tau}+k_2'y$, and $\sigma=k_1'Ut+k_2'y$. At the flame front where $x_c=Ut$ and $x_b=(U-V)t$, $\eta_c=\eta_b=0$, the attenuation factors $e^{-\eta_c}$ and $e^{-\eta_b}$ are 1, and the arguments of the disturbance waves have the form $(k_1'Ut+k_2'y)$.

The procedure of reference 23 is utilized in reference 22 to treat a similar interaction problem for consideration of flame-front stability. It is assumed that there are first-order perturbations in the laminar flame speed U (in the present notation). Reference 22 presents results only for the special case where the plane of polarization of the incident shear wave is in the plane $x_{1,c}-x_{2,c}(\theta=0°)$ and the wave-number vector is parallel to the unperturbed flame front ($\varphi=90°$). The results of the present analysis were compared with those of reference 22 for the case of an absence of first-order perturbations in the laminar flame speed and for the special case of $\theta=0°$ and $\varphi=90°$ without heat-release perturbations. Although agreement as to sign and magnitude is obtained for the shear-field velocity components, apparently differences in sign occur for the potential-field velocity-component amplitudes as indicated in the following table:

	Present analysis	Analysis of ref. 22
$\frac{u_{p,c}'}{U}$	$-A$	$-A$
$\frac{i'_{p,c}}{U}$	iA	$-iA$
$\frac{u_{p,b}'}{U}$	A	$-A$
$\frac{v_{p,b}'}{U}$	iA	iA

Consideration of conservation of momentum across the flame front indicates that $v_{p,c}'/U$ and $v_{p,b}'/U$ should be of the same sign. The present analysis is in agreement with this consideration.

REFERENCES

1. Damköhler, Gerhard: The Effect of Turbulence on the Flame Velocity in Gas Mixtures. NACA TM 1112, 1947.
2. Shelkin, K. I.: On Combustion in a Turbulent Flow. NACA TM 1110, 1947.
3. Bollinger, Lowell M., and Williams, David T.: Effect of Reynolds Number in the Turbulent-Flow Range on Flame Speeds of Bunsen Burner Flames. NACA Rep. 932, 1949. (Supersedes NACA TN 1707.)
4. Williams, G. C., Hottel, H. C., and Scurlock, A. C.: Flame Stabilization and Propagation in High Velocity Gas Streams. Third Symposium on Combustion and Flame and Explosion Phenomena, The Williams & Wilkins Co. (Baltimore), 1949, pp. 21–40.
5. Markstein, G. H.: Interaction of Flame Propagation and Flow Disturbances. Third Symposium on Combustion and Flame and Explosion Phenomena, The Williams & Wilkins Co. (Baltimore), 1949, pp. 162–167.
6. Karlovitz, Béla, Denniston, D. W., Jr., and Wells, F. E.: Investigation of Turbulent Flames. Jour. Chem. Phys., vol. 19, no. 5, May 1951, pp. 541–547.
7. Scurlock, A. C., and Grover, J. H.: Propagation of Turbulent Flames. Fourth Symposium (International) on Combustion, The Williams & Wilkins Co. (Baltimore), 1953, pp. 645–658.
8. Westenberg, Arthur A.: Flame Turbulence Measurements by the Method of Helium Diffusion. Jour. Chem. Phys., vol. 22, no. 5, May 1954, pp. 814–823.
9. Wohl, K., Shore, L., Von Rosenberg, H., and Weil, C. W.: The Burning Velocity of Turbulent Flames. Fourth Symposium (International) on Combustion, The Williams & Wilkins Co. (Baltimore), 1953, pp. 620–635.
10. Batchelor, G. K.: The Theory of Homogeneous Turbulence. Cambridge Univ. Press, 1953.
11. Carrier, G. F., and Carlson, F. D.: On the Propagation of Small Disturbances in a Moving Compressible Fluid. Quarterly Appl. Math., vol. 4, no. 1, Apr. 1946, pp. 1–12.
12. Moore, Franklin K.: Unsteady Oblique Interaction of a Shock Wave with a Plane Disturbance. NACA Rep. 1165, 1954. (Supersedes NACA TN 2879.)
13. Clark, Thomas P., and Bittker, David A.: A Study of the Radiation from Laminar and Turbulent Open Propane-Air Flames as a Function of Flame Area, Equivalence Ratio, and Fuel Flow Rate. NACA RM E54F29, 1954.
14. Dugger, Gordon L.: Effects of Initial Mixture Temperature on Flame Speed of Methane-Air, Propane-Air, and Ethylene-Air Mixtures. NACA Rep. 1061, 1952. (Supersedes NACA TN's 2170 and 2374.)
15. Moyal, J. E.: The Spectra of Turbulence in a Compressible Fluid; Eddy Turbulence and Random Noise. Proc. Cambridge Phil. Soc., vol. 48, pt. 2, Apr. 1952, pp. 329–344.
16. Ribner, H. S.: Shock-Turbulence Interaction and the Generation of Noise. NACA TN 3255, 1954.
17. Ribner, H. S., and Tucker, M.: Spectrum of Turbulence in a Contracting Stream. NACA Rep. 1113, 1953. (Supersedes NACA TN 2606.)
18. Morse, Philip M.: Vibration and Sound. Second ed., McGraw-Hill Book Co., Inc., 1948.
19. Hottel, H. C., Williams, G. C., and Satterfield, C. N.: Thermodynamic Charts for Combustion Processes, pt. I. John Wiley & Sons, Inc., 1949.
20. Gerstein, Melvin, Levine, Oscar, and Wong, Edgar L.: Fundamental Flame Velocities of Pure Hydrocarbons. I - Alkanes, Alkenes, Alkynes, Benzene, and Cyclohexane. NACA RM E50G24, 1950.
21. Levine, Oscar, and Gerstein, Melvin: Fundamental Flame Velocities of Pure Hydrocarbons. III - Extension of Tube Method to High Flame Velocities - Acetylene-Air Mixtures. NACA RM E51J05, 1951.
22. Markstein, George H.: Interaction of a Plane Flame Front with a Plane Sinusoidal Shear Wave. Jour. Aero. Sci., vol. 20, no. 8, Aug. 1953, pp. 581–582.
23. Ribner, H. S.: Convection of a Pattern of Vorticity Through a Shock Wave. NACA Rep. 1164, 1954. (Supersedes NACA TN 2864.)